Geochemistry of the Ultramafic Rocks from the Bay of Island Ophiolitic Complex, Newfoundland.

Fabio Gianotti Stern, B.Sc.

Thesis submitted to the Faculty of Graduate and Postdoctoral Studies in partial fulfillment of the requirements for the degree of M.Sc. in Earth Sciences

Ottawa-Carleton Geoscience Centre
Department of Earth Sciences
University of Ottawa
Ottawa, Canada

January 2013

THESIS ABSTRACT

The Bay of Islands Ophiolitic Complex (BOIC) is one of most well preserved and well-exposed ophiolites in the world. The BOIC consist of four massifs; these are the Table Mountain (TBL), North Arm Mountain (NAM), Blow-Me-Down Mountain (BMD) and Lewis Hills massifs. Proposed geological environments of the BOIC in Newfoundland are diverse; ranging from oceanic spreading ridge to supra-subduction setting.

The BOIC has a complete ophiolite sequence as defined at the Penrose Conference (Anonymous, 1972) including ultramafic mantle rocks, ultramafic to gabbroic cumulate rocks, sheeted dikes, pillowed basaltic rocks and capping sedimentary rocks in structurally ascending order. We studied harzburgite and overlying massive dunite in the BOIC. Harzburgite is generally medium-grained, and contains olivine, orthopyroxene, Cr-spinel, clinopyroxene and rare sulfide minerals. Harzburgite is massive to strongly deformed, with local development of mylonitic shear zones. A foliation and lineation are defined by elongated and fragmented grains of orthopyroxene and Cr-spinel. Dikes, sills, veins, and irregularly-shaped bodies of dunite and pyroxenite are present throughout the harzburgite unit.

Dunite is the predominant lithology of the Blow-Me-Down Mountain. It is typically fine- to medium-grained, massive, and contains minor Cr-spinel and rare sulfide minerals. Dunite contains olivine, Cr-spinel and minor pyroxenes in some samples. Olivine crystals are commonly partly replaced by serpentine along fractures and in outer rims.

Bulk rock and mineral composition data suggest that harzburgites are mild to highly refractory mantle residues after partial melting. In contrast all dunite samples show a

cumulate geochemical signature from a mafic melt that originated from highly refractory mantle peridotites.

Our study suggest that the harzburgite in the BOIC originally formed as oceanic lithosphere at a slow spreading ridge, possibly in the vicinity of active arc systems, whereas the parental melt for dunites formed in subduction setting.

The second part of this study measured trace element compositions for olivine, Cr-spinel and bulk rock of dunite. The measured bulk rock compositions are compared to those of calculated based on mineral chemistry and their abundance. This comparison suggests that the trapped melt fraction was negligible during the crystallization of the dunites. The calculated melt compositions for the dunites confirm that the melt formed in subduction setting.

RÉSUMÉ DE THESE

Le Complexe Ophiolitique de Bay of Island (COBI) est un example d'ophiolite exposés les mieux préservés au monde. Le COBI est constitué de quatre massifs; du nord au sud on retrouve les massifs Table Mountain (TBL), North Arm Mountain (NAM), Blow-Me-Down Mountain (BMD) et Lewis Hills. Les explications relatives aux origines du COBI de Terre-Neuve varient depuis la formation en falaise des linosphères océaniques jusqu'à l'environnement de zones de supra-subductions.

Le COBI présente une séquence ophiolitique complète, telle que définie par les participants de la conférence de Penrose (Anonymes, 1972), incluant, en ordre ascendant, une couche de roche accumulée de l'ultramafique au gabbroique, digues en feuille, coussins de roche basaltique et couverture de roche sédimentaire. Nous avons étudié l'harzburgite et les dunite massives de recouvrement du COBI.

L' harzburgite est généralement de grain moyen avec des textures variant de massives à fortement déformées, avec des développements locaux de zones de clivage mylonitique. Les harzburgites typiques présente une foliation et lineation définie par des grains allongés et fragmentés d'orthopyroxène et de Cr-spinel. On note la présence à travers toute la formation de harzburgite, de digues, de seuils de veines et de formations de dunite et de pyroxenite irrégulières. L'harzburgite contiens de l'olivine, de l'orthopyroxène, du Cr-spinel, du clinopyroxène et des sulfites minéraux.

La dunite, depuis le grain fin jusqu'au grain moyen, est la lithologie prédominante dans le Blow-Me-Down Mountain. Elle contient un peu de Cr-spinel. Certains échantillons de dunite contiennent de l'olivine, du Cr-spinel et un peu de pyroxène. Les cristaux d'olivine sont souvent remplacés par des serpentines.

Les données relatives aux blocs de roches et les calculs de valeurs fO_2 démontrent que l'harzburgite est formée de résidus réfractaires du manteau ayant subit une fonte partielle. Par contre, tous les échantillons de dunite expriment une caractéristique cumulat.

Notre étude suggère que l'harzburgite du COIB est, à l'origine, une formation en falaise litosphérique océanique de propagation lente, possiblement dans le voisinage de systèmes d'arc actifs.

Cette étude a aussi mesuré et comparé l'abondance d'éléments traces provenant des roches dunitiques la composition en trace provenant d'une analyse de minéraux. Cette comparaison nous a permis d'évaluer la fraction liquide piégé et la composition du liquide en équilibre avec la dunite du Complexe Ophiolitique de Bay of Islands.

Acknowledgements

I would like to thank my thesis supervisor, Dr. Kéiko Hattori, for all her support and specially encouragement and availability during these two years. Her enthusiasm and dedication were essential and really important during the project and also during the fieldwork that we conducted in the island of Newfoundland under very cold weather in the Fall of 2010.

I would also like to thank Jéan Bedard, who helped me since the begining of the project and whose expertize on the study area was fundamental to the completion of this MSc. Without him, we would probably still be lost in the Blow-Me-Down massif.

This project was funded in part by the **Discovery Grant** Natural Science and Engineering Research Council of Canada to Keiko Hattori. I would like to acknowledge the Travel Grants from GSAED and FGPS of the University of Ottawa that helped make possible the presentaion of this research at the Geological Society of America Meeting in 2011.

Furthermore, I wish to thank Peter Jones and Glenn Poirer who provided many hours of help and guidance during the microprobe analysis. Dr. Nimal De Silva and Smitha Mohanty also provided analytical and laboratory assistance, and George Mrazek provided thin sections. Tara Kell provided XRF analyses and help with XRD and Wilfredo Diegor of the Memorial University of Newfoundland for his assistance with the LA-ICP-MS analysis.

My geologist friends provided many hours of good times, and intellectual support over the past two years, which also helped me a lot. I would especially like to thank Jason Duff, Dave Lowe and Fritz Griffith. Special thanks to all my family for the unconditional love and support at all times.

TABLE OF CONTENTS

LIST OF FIGURES

Chapter 01

Chapter 01

LIST OF TABLES

Chapter 01

Chapter 02

LIST OF APPENDIX

Appendices are found on CD attached to this thesis

INTRODUCTION

Preamble

The term ophiolite was first introduced by Alexander Brongniart (1813) for an assemblage of green rocks in the Alps (serpentine, diabase). Gustav Steinman (1856-1929) elevated the term “ophiolite” to a new concept. Steinman interpreted these rocks from the Alps as differentiated magmatic rocks evolved on the ocean floor. This interpretation led to the "Steinmann's trinity", consisting of serpentinites, diabase and chert.

Harry H. Hess in 1955 argued about an island arc origin of mafic-ultramafic rock assemblages and serpentinized peridotites found in orogenic belts. Hess also combined his observations from the Appalachian and Caribbean peridotites with post-war developments in marine geological and geophysical investigations to suggest that the ocean floor was extensively serpentinized by waters rising out of the mantle.

This ophiolites discussion led to the organization of an international Penrose Field Conference in September 1972. Participants of this conference made field observations in various ophiolite complexes in the western United States, discussed the European ophiolite concept and the ocean crust–ophiolite analogy, and produced a consensus statement on the definition of an ophiolite (Anonymous, 1972).

The origin of ophiolites has still been in debate for a long time. Proposed opinions include the exposed oceanic lithosphere formed at ridges, a mixture of oceanic lithosphere and igneous rocks formed in subduction zones. The Bay of Islands Ophiolitic Complex (BOIC) in Newfoundland is one of the three major ophiolites in the world. Similar to many other ophiolites, the origin of the BOIC has been controversial.

This study discusses the BOIC evolution, based on new data on mineral-chemistry, major and trace elements, and PGE abundance for ultramafic rocks with a special focus on the Blow-Me-Down massif. Combining all data, we suggest that the harzburgite in the BOIC originally formed as oceanic lithosphere at a slow spreading ridge, possibly in the vicinity of active arc systems. Subduction initiation resulted in flux-melting at high fO_2 to form melts to form ultramafic cumulates.

This study also reports the concentrations of a suite of minor and trace elements in cumulate dunites from BOIC, using laser ablation coupled to a mass spectrometer. The report further evaluates the melt fraction of cumulate rocks based on trace element abundance, including rare earth elements, of constituent minerals and bulk rocks.

PREVIOUS WORK

Proposed origins of the Ordovician age Bay of Island Ophiolitic Complex (BOIC) in Newfoundland are diverse including the oceanic lithosphere formed at a ridge and arc lithosphere. The BOIC consist of four massifs; these are the Table Mountain (TBL), North Arm Mountain (NAM), Blow-Me-Down Mountain (BMD) and Lewis Hills massifs. The BOIC is tectonically juxtaposed to the west against a complex assemblage of metamorphosed and deformed ophiolitic rocks referred to as the Coastal Complex (CC) (Williams 1973).

In one of the first studied about BOIC, Snelgrove et. al (1934) conducted reconnaissance mapping of BMD mountain. Smith (1958) proposed BOIC origin as a syntectonic layered intrusion, after mapping the North Arm Mountain massif. Williams (1973) generated the first maps covering the entire BOIC and interpreted it as oceanic lithosphere. Karson and Dewey (1978) and Suhr and Cawood (2001) suggested the Coastal Complex, a complex assemblage of metamorphosed and deformed ophiolitic rocks, were accreted against oceanic lithosphere of the BOIC along an oceanic transform fault. Searle

and Stevens (1984) concluded that the Coastal Complex was significantly older than the BOIC, and proposed a back-arc spreading origin for the BOIC. The proposed interpretation of the relationship of the two is supported by geochronological data. The U/Pb zircon ages of 505 Ma +3/-2 for the Little Port Assemblage of the Coastal Complex (Jenner et al., 1991) and of 500.6 +/- 2 Ma and 503.7 +/- 3.2 Ma of the western part of the Lewis Hills massif (Kurth et al., 1998) are significantly older than those of the BOIC. The latter include an U/Pb zircon age for a BMD trondhjemite of 485.7 Ma +1.9/-1.2 (Dunning and Krogh, 1985); a zircon age of 484 +/- 5 Ma for a BMD gabbro (Jenner et al., 1991), and an apatite age of 485+/-1 Ma from a gabbro in the eastern Lewis Hills (Kurth et al., 1998).

Suen et al. (1979) and Casey et al. (1985) determined major- and trace element compositions of gabbroic rocks and documented that the geochemical signatures including low light REEs are similar to those of mid-oceanic ridge basalts, and concluded that they formed at oceanic ridges. Elthon et al. (1982, 1984) proposed that the ultramafic cumulates represent high-pressure crystallization of melts parental to the more evolved gabbroic rocks. In contrast, Bédard (1991, 1993) and Bédard and Hébert (1996) proposed that the ultramafic cumulates formed from an underplating sill complex, and suggested a boninitic affinity based on the high Cr# (Cr/Cr+Al) of Cr-spinel and low Ti-content of pyroxenes. Jenner et al. (1991), Elthon (1991) suggested that the gabbroic intrusions and volcanic rocks of the BOIC formed in a supra-subduction-zone environment based on trace element signatures of dioritic and basaltic rocks.

Trace element studies in cumulate rocks are important to understand their chemistry and allow determining the concentration of elements in the liquids that coexisted with the rocks at the time of crystallization. There are not many trace element studies about cumulate plutonic rocks. Bédard (1994) using bulk rock trace element analyses obtained the

equilibrium distribution of trace elements of cumulates rocks, and the concentration of trace elements in the coexisting liquids. In the same year Paktunc and Cabri (1994) analyzed by proton and electron microprobes Cr- spinels from a number of localities to examine the variation of trace elements in different geological environments, including dunite and chromitites from BOIC. Almost 15 years later, three new different studies about trace element concentrations in cumulate rocks/ultramafic rocks were published. Dare et al. (2009) studied Cr–spinel from 58 peridotites from oceanic and ophiolitic settings with the objective of further develop the tectonic discrimination of peridotites from mid-ocean ridges (MOR) and supra-subduction zone (SSZ) settings.

De Hoog et al. (2009) studied trace-element compositions of olivine from 75 mantle rocks of diverse origin, including xenoliths from kimberlites, basaltic lavas and orogenic peridotites. They were determined by laser ablation ICP-MS with the objective of identifying systematic variations between mantle lithologies.

The most recent and complete study about trace element in Cr-spinel from cumulate rocks was presented by Pagé and Barnes (2009). This study presents the concentrations of a complete suite of minor and trace elements (Sc, Ti, V, Mn, Co, Ni, Zn, and Ga) in Cr-spinel from podiform chromitites of the Thetford Mines Ophiolite (Canadian Appalachians) and from the associated boninite lavas, using laser ablation inductively coupled to a plasmaquadrupole mass spectrometer.

THESIS OBJECTIVES

Ophiolites have brought together diverse groups of international scientists far more than any other topic in geology. The ophiolites studies and debates helped to form the nucleus of the tectonics hypothesis, which was formulated as quantitative theory in 1967-1968. The main objective of this thesis is to provide new mineral-chemical, whole-rock, and PGE data for the ultramafic rocks from BOIC, with a special focus on the Blow-Me-Down massif, which has received less attention than the other massifs in the past.

This thesis also addresses a geochemical study about trace elements in the dunites from the Blow-Me-Down massif from BOIC. Trace element concentration were measured in olivine and Cr-spinel and bulk rock using LA-ICP with the objective of obtaining the chemistry signature of the cumulate dunites from BOIC and the melt in equilibrium with them.

THESIS OUTLINE

This thesis is presented as two papers (chapters 1 and 2), all of which were written to address independent themes of this study. This method of presentation involves undesirable redundancies, especially with respect to analytical procedures, petrography and some geochemical results.

Chapter 1 is a paper focused in constraining the tectonic evolution of the Bay of Island Ophiolitic Complex. The manuscript will be submitted to a refereed journal.

Chapter 2 is a report focusing on trace element composition of dunites from Blow-Me-Down and is not written with intent of publication in a refereed journal.

STUDY AREA

The Bay of Island Ophiolitic Complex, western Newfoundland, was selected for this study because of its excellent exposure and convenient accessibility. The island of Newfoundland is part of the Appalachian-Caledonian orogenic belt which is known by numerous ophiolites occurrences (Fig. i). Newfoundland is divided into four tectonic zones from east to west these are the Avalon, Gander, Dunnage, and Humber Zones. The Dunnage Zone has been subdivided by Williams et al. (1988) into two major subzones; the Notre Dame subzone to the West and the Exploits subzone East of the Red Indian Line. This division reflects marked differences in stratigraphy and fauna in Lower to Middle Ordovician rocks.

The BOIC is a klippe of Notre Dame Subzone oceanic rocks that was emplaced on the collapsed passive margin of North America during the Ordovician Taconian orogeny (Cawood and Suhr, 1992).

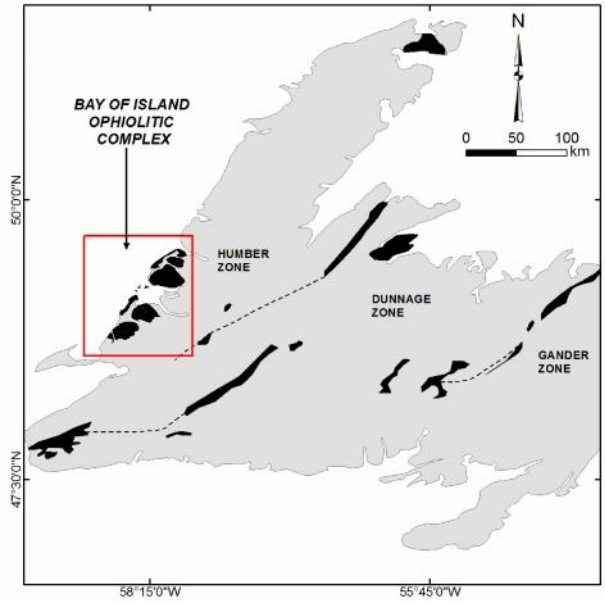

Figure i: Ophiolitic complexes of the Newfoundland Appalachians (black). Modified after Dunning and Chorlton (1985).

The BOIC consist of four massifs; from north to south these are the Table Mountain (TBL), North Arm Mountain (NAM), Blow-Me-Down Mountain (BMD) and Lewis Hills massifs (Fig. ii). Each massif contains mantle and crustal rocks. The BOIC is tectonically juxtaposed to the west against the Costal Complex (CC), which is an assemblage of metamorphosed and deformed igneous and sedimentary rocks (Karson, 1984).

Among the four massifs, North Arm Mountain and Blow-Me-Down Mountain contain nearly complete ophiolite sequences as defined by the Penrose Conference Participants (Anonymous, 1972) including ultramafic rocks, ultramafic to gabbroic lower crust, sheeted dikes, pillowed basaltic rocks and capping sedimentary rocks in structurally ascending order. The Table Mountain massif and the eastern half of the Lewis Hills massif only preserve the lower parts of the sequence. The Lewis Hills has been interpreted to represent a transform / spreading ridge junction, with the eastern part belonging to the BOIC (Karson, 1984).

This study focus on ultramafic rocks from BOIC, collected after mapping in September, 2010 from the Table Mountain, and Blow-Me-Down Mountains. Samples from North Arm Mountain are those reported by Bédard and Hébert (1998).

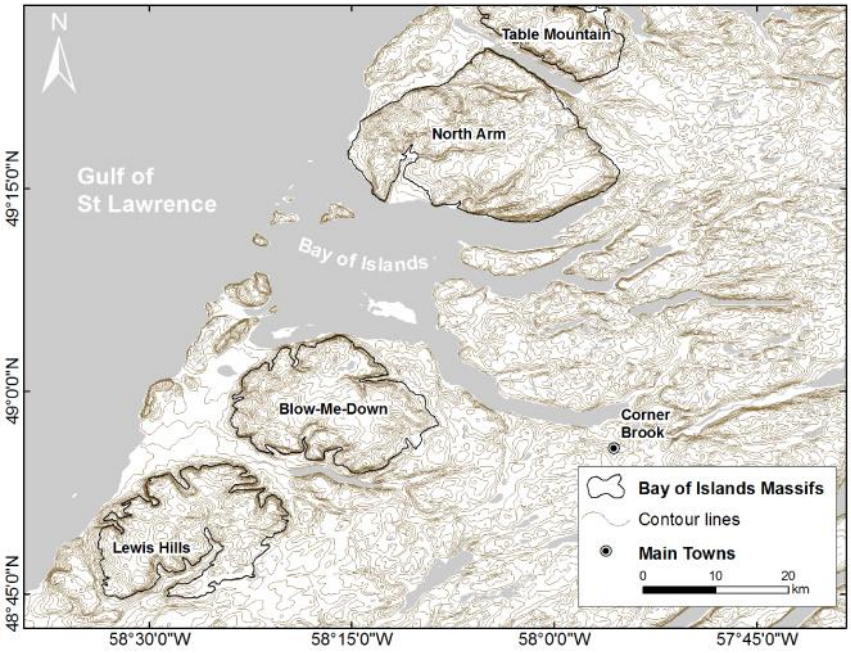

Figure ii: Topographic map of the Bay of Island Ophiolitic Complex.

STATEMENT OF ORIGINAL CONTRIBUTION

The Bay of Island ophiolite Complex is one of the best preserved and exposed ophiolites in the world. Although the Complex has been studied, its paleotectonic setting remains controversial. This manuscript presents new data of mineral chemistry, whole-rock and trace element chemistry, and PGE abundance for ultramafic rocks and the spatial variation of spinel chemistry. Our samples include rocks from the Blow-Me-Down massif, which has few information, and fill an important gap in coverage of data of the BOIC.

The study involved a week of fieldwork in the BOIC, Newfoundland in September 2010. Samples collected by Drs. Jean Bédard and Rejéan Hébert in 1998 were also used for comparison purpose in this study.

The geochemical data, mineral analyses, petrological observations, along with all interpretations, are the result of my original work. Chapter 1 "*Constraining the tectonic*

evolution of the Bay of Island Ophiolitic Complex, Newfoundland" was orally presented in the Geological Society of America Meeting, 2011 in Minneapolis (Appendix E).

All two chapters benefited from edits, comments and suggestions from Dr. Keiko Hattori. Chapter 1 benefited from edits and comments also from Dr. Jean Bédard.

Chapter 1

Constraining the tectonic evolution of the Bay of Islands Ophiolitic Complex, Newfoundland.

Fabio Stern[1], Keiko Hattori[1], and Jean H. Bédard[2]
[1]*Department of Earth Sciences, University of Ottawa, 140 Louis Pasteur, Ottawa, Ontario, K1N 6N5, Canada.*
[2]*Geological Survey of Canada, 490 de la Couronne, Québec, QC, G1K 9A9, Canada.*

ABSTRACT

Proposed origins of the Bay of Island Ophiolitic Complex (BOIC) of Ordovician age in Newfoundland are diverse; ranging from oceanic lithosphere formed at a ridge to a supra-subduction zone environment. We studied harzburgite and overlying massive dunite in the BOIC, with a special focus on the Blow-Me-Down massif, which has received less attention than the other massifs in the past. Cr-spinel in BOIC harzburgite shows a continuous variation in Cr# (Cr/Cr+Al) from 0.32 to 0.64 and XMg (Mg/Mg+Fe^{2+}) from 0.52 to 0.70. Forsterite (Fo) contents of olivine range from 90 to 91 and NiO from 0.34 to 0.42 wt%. Mineral pairs of harzburgites in BOIC plot in moderately fertile to refractory mantle in the olivine-spinel mantle array (OSMA) of Arai (1994). In a Cr# vs. XMg diagram, low Cr # spinels compositions overlap the fields for abyssal and subarc mantle peridotite, whilst those with high Cr# extend into the forearc mantle field.

Cr-spinel in dunite has Cr# ranging from 0.16 to 0.69 and XMg from 0.47 to 0.75. The Fo contents (86 to 91) in olivine extend to lower values than those of harzburgite. The platinum group element (PGE) contents in dunite show a slightly positively sloped primitive-mantle normalized pattern with low Os and Ir, indicating that these dunites are cumulates from a mafic melt, not ultra-restites. Values of Cr# for spinel in dunite suggest that the source mantle for its parental melt was refractory, similar to forearc mantle, indicating the progressive depletion in the mantle during the evolution of the BOIC.

Combining all data, we suggest that the harzburgite in the BOIC originally formed as oceanic lithosphere at a slow spreading ridge, possibly in the vicinity of active arc systems. Subduction initiation resulted in flux-melting at high fO_2 to form melts to form ultramafic cumulates. The Blow-Me-Down massif is mostly composed of very thick (~ 3 km) dunites. The next massif to the north, at North Arm, has much thinner dunites and contains significant

proportions of pyroxenite and pyroxene-bearing peridotite. The northernmost massif at Table Mountain has a very thin dunite, recording progressive fractionation as the magma spread beneath gabbroic rocks of oceanic origin.

INTRODUCTION

The Bay of Islands Ophiolitic Complex (BOIC) of the western Newfoundland Appalachians has remarkable preservation of all components of a typical Penrose ophiolite stratigraphy (Anonymous, 1972). The origin and evolution of this ophiolite has been debated extensively over the last 30 years (Suen et al., 1979; Casey et al., 1985; Bédard, 1991; Elthon, 1991; Jenner et al., 1991; Cawood and Suhr, 1992; Kurth et al., 1998; Suhr and Cawood, 2001; Zagorevski and van Staal, 2011).

While structural and stratigraphic evidence provides important constraints on the origin of ophiolites, the commonest approach is to use the geochemical systematics of the rocks found in these complexes and to compare them to similar rocks of known settings. Although many different tectonic models have been proposed for the BOIC (Elthon, 1991; Jenner et al., 1991, Kurth et al., 1998, 2004), we present here new data on mineral-chemistry, major and trace elements, and PGE abundance for ultramafic rocks which show that one tectonic setting. We also provide new data from the Blow-Me-Down massif, compare these to data from the other massifs and discuss the BOIC evolution.

Many ophiolites have dunite sandwiched between refractory mantle harzburgite and gabbros, and there is a debate whether these dunites represent ultra-depleted mantle peridotites, or cumulate rocks. Our data will show that these dunites are cumulate rocks.

GEOLOGY

Regional Geology

Newfoundland is divided into four tectonic zones. From East to West these are the Avalon, Gander, Dunnage, and Humber Zones. The Dunnage Zone has been subdivided by Williams et al. (1988) into two major subzones; the Notre Dame subzone to the West and the Exploits subzone East of the Red Indian Line. This division reflects marked differences in stratigraphy and fauna in Lower to Middle Ordovician rocks.

The BOIC is a klippe of Notre Dame Subzone oceanic rocks that was emplaced on the collapsed passive margin of North America during the Ordovician Taconian orogeny (Cawood and Suhr, 1992).

The BOIC consist of four massifs; from North to S outh these are the Table Mountain (TBL), North Arm Mountain (NAM), Blow-Me-Down Mountain (BMD) and Lewis Hills massifs. Each massif contains mantle and crustal rocks. The BOIC is tectonically juxtaposed to the west (Fig. 1) against the Coastal Complex which is an assemblage of metamorphosed and deformed igneous and sedimentary rocks including an old arc complex (Karson, 1984). The Lewis Hills massif contains the magmatic contact between Coastal Complex and the BOIC (Karson & Dewey, 1978; Cawood & Suhr, 1992; Kurth et al., 1998).

Among the four massifs, NAM and BMD contain nearly complete ophiolite sequences as defined by the Penrose Conference Participants (Anonymous, 1972) including ultramafic mantle rocks, ultramafic to gabbroic cumulate rocks, sheeted dikes, pillowed basaltic rocks and capping sedimentary rocks in structurally ascending order. The TBL and the eastern half of the LH only preserve the lower parts of the sequence (Fig. 1).

Snelgrove et. al (1934) conducted reconnaissance mapping of BMD mountain. Smith (1958) mapped the North Arm Mountain massif and proposed its origin as a syntectonic

layered intrusion. Williams (1973) generated the first maps covering the entire BOIC and interpreted it as oceanic lithosphere. Karson and Dewey (1978) and Suhr and Cawood (2001) suggested the rocks of the Coastal Complex were accreted against oceanic lithosphere of the BOIC along an oceanic transform fault. Searle and Stevens (1984) concluded that the Coastal Complex was significantly older than the BOIC, and proposed a back-arc spreading origin for the BOIC. The proposed interpretation of the relationship of the two is supported by geochronological data. The U/Pb zircon ages of 505 Ma +3/-2 for the Little Port Assemblage of the Coastal Complex (Jenner et al., 1991) and of 500.6 +/- 2 Ma and 503.7 +/- 3.2 Ma of the western part of the Lewis Hills massif (Kurth et al., 1998) are significantly older than those of the BOIC. The latter include an U/Pb zircon age for a BMD trondhjemite of 485.7 Ma +1.9/-1.2 (Dunning and Krogh, 1985); a zircon age of 484 +/- 5 Ma for a BMD gabbro (Jenner et al., 1991), and an apatite age of 485+/-1 Ma from a gabbro in the eastern Lewis Hills (Kurth et al., 1998).

Mid ocean ridge setting for the formation of BOIC was proposed by Suen et al. (1979) and Casey et al. (1985), based on the similar major and trace element compositions of BOIC gabbroic rocks to mid-oceanic ridge basalts. Elthon et al. (1982, 1984) proposed that the ultramafic cumulates represent high-pressure crystallization of melts parental to the more evolved gabbroic rocks. In contrast, Bédard (1991, 1993) and Bédard and Hébert (1996) proposed that the ultramafic cumulates formed from an underplating sill complex, and suggested a boninitic affinity based on the high Cr# (Cr/Cr+Al) of Cr-spinel and low Ti-content of pyroxenes. This suggestion appears to be consistent with trace element inversion calculations on dunites, orthopyroxenites and wehrlites (Bédard, 1994, 2007). Jenner et al. (1991), Elthon (1991) suggested that the gabbroic intrusions and volcanic rocks of the BOIC formed in a supra-subduction-zone environment based on trace element signatures of dioritic

and basaltic rocks. The weak subduction-related geochemical signature of tholeiitic igneous rocks and abundant sheeted dykes, together with the age relationships, suggest that the BOIC may have formed as a peri-continental marginal basin (e.g. Cawood & Suhr, 1992).

Samples

Representative samples of ultramafic rocks were collected after mapping in September, 2010 from the Table Mountain, and Blow-Me-Down Mountains. Samples from North Arm Mountain are those reported by Bédard and Hébert (1998). Weathered surface was removed in the field. Hydration of olivine and orthopyroxene forms serpentine and magnetite and other hydrous phases, such as talc and brucite (Komor et al., 1985). Serpentine forms also narrow veinlets (<0.05 mm) in rocks. Fine-grained dusty magnetite is commonly disseminated within serpentine; and magnetite also forms discontinuous veinlets along grain boundaries and fractures of silicate minerals. High-temperature metasomatic minerals, such as phlogopite and amphiboles, were not observed. Although it is possible that very minor amounts of these phases may have been present, it is unlikely that such metasomatic phases are significant considering that harzburgite rocks are essentially anhydrous and retain the primary textures.

Rock Types

Harzburgite

Harzburgite is the tectonically lowest igneous unit in the ophiolite sequence in the BOIC (Fig. 1). The thickest and most complete sections are exposed in the TBL and NAM massifs (e.g. Suhr, 1992). It is generally medium-grained, and ranges from massive to strongly deformed, with local development of mylonitic shear zones. Typical harzburgites show a foliation and lineation defined by elongated and fragmented grains of orthopyroxene

and Cr-spinel. Dikes, sills, veins, and irregularly-shaped bodies of dunite (Fig. 2) and pyroxenite are present throughout the harzburgite unit (Varfalvy et al., 1997) with sharp contacts with the host harzburgite and there is no obvious metasomatic effects on harzburgite. Vein thicknesses vary from thin (< 10 cm) to metric in size, and some veins are folded.

Harzburgite contains olivine (70 - 80 vol.%), orthopyroxene (17- 30 vol.%), Cr-spinel (< 1 vol.%) and minor clinopyroxene and sulfide minerals. Orthopyroxene occurs as coarse subhedral grains (< 0.8 mm, up to 2 mm). Harzburgite in NAM contains subhedral to anhedral porphyroclasts of orthopyroxene, and some form aggregates (~10 mm) of smaller grains (< 3 mm). Orthopyroxene may contain inclusions of olivine and rare Cr-spinel. Olivine is generally medium to fine-grained (< 0.5 mm), anhedral, and only rarely contains Cr-spinel or sulfide inclusions

Cr-spinel is anhedral to subhedral (Fig. 3a). Grains are small, less than 0.2 mm in most cases with rare coarse grains reaching 0.6 mm. It is red-brown to opaque in thin sections under transmitted light, and commonly rimmed by secondary magnetite. Cr-spinel occurs along grain boundaries of olivine or as rare inclusions in orthopyroxenes and clinopyroxene.

Clinopyroxene is rare (less than 5 vol.%). The grains are subhedral and generally smaller than 1.5 mm. Clinopyroxene commonly occurs near orthopyroxene grains, it may occur in contact with olivine and Cr-spinel.

Rare pyrrhotite with minor chalcopyrite or pentlandite are disseminated as small (< 200 μm) angular grains along grain boundaries of silicate minerals (Fig. 3c). Sulphur contents of bulk rocks (9 to 239 ppm S) show a broad positive correlation with Cu contents (Fig. 4), confirming that chalcopyrite hosts most of the Cu. The atomic ratios of Cu to S are lower than 0.5, suggesting that most of the S is hosted by Fe sulfides.

Dunite

Dunite is the predominant lithology of the Blow-Me-Down Mountain. It is well exposed on the flank near the top and on the flat top (~ 10 x 5 km in size) of the mountain. Dunite is typically fine- to medium-grained, massive, and contains minor Cr-spinel. In some location dunite rocks show layers of Cr-spinel-rich bands (Fig. 5). At some locations dunite displays a weak foliation defined by elongated grains of Cr-spinel and lenses of aggregates of Cr-spinel. Dunite contains olivine (> 96 vol.%), Cr-spinel (< 1.5 vol.%) and minor pyroxenes in some samples. Olivine crystals are medium to fine-grained (< 0.4 mm) and subhedral. Olivine is commonly partly replaced by serpentine, which is reflected by high values (11.4-16.8 wt.%) of loss on ignition (LOI; Table 4).

Cr-spinel abundance in dunite is typically greater than that of harzburgite. They occur along grains boundaries and as inclusion in olivine. The Cr-spinel grains are usually small (< 0.2 mm) and opaque in thin sections under transmitted light, with secondary magnetite rims (Fig. 3b). Rare coarse Cr-spinel forms anhedral to subhedral grains. Elongated grains were also observed in some samples.

Sulfide minerals are common in dunite (up to 894 ppm S). The majority of sulfide grains form angular to globular grains ranging in size from <100 μm to 500 μm at grain boundaries or at triple junctions of olivine grains. They are commonly replaced by Fe oxides leaving isolated relict sulfides (Fig. 3d). Although high-temperature sulfide melt may dissolve up to 50% oxygen at moderately high fO_2 around the quartz-magnetite-fayalite buffer (Francis, 1990), the texture and abundance of Fe oxide in many sulfide grains from the BOIC are interpreted to be the result of low temperature oxidation. The evidence suggests that the original concentrations of S are higher than the observed values. The sulfide minerals

are mostly high Ni pyrrhotite (31 to 41 wt% Ni) with minor chalcopyrite and pentlandite. The original Ni contents of pyrrhotite may have been lower because of the oxidation of sulfides with little Ni in Fe oxide. Exsolution textures are recognized in the less oxidized grains, where patches of pentlandite exsolve from pyrrhotite, and rare heazlewoodite exsolves from pentlandite. Sulfide minerals are also found as rare inclusions in olivine and Cr-spinel. These are small (less than 10 μm), globular or angular inclusions (pentlandite, pyrrhotite and chalcopyrite). Globular shaped sulfides were likely formed as immiscible sulfide melt at high temperatures. Thus, the textural evidence suggests that the sulfides in BOIC dunites likely formed from high temperature sulfide melts, and later unmixed during cooling, and that they have undergone later oxidation at low temperatures.

Wehrlite

Wehrlite forms veins of varying width (up to 30 cm) cutting dunite. Wehrlite is coarse-grained, contains olivine (> 80 vol.%), clinopyroxene (< 20 vol.%) and minor Cr-spinel (< 1 vol.%). Olivine grains are large (~ 1 mm) and subhedral, and commonly hydrated to form serpentine pseudomorphs. Clinopyroxene is mostly anhedral and large (~ 2 mm). Some form aggregates up to 8 mm in size. Clinopyroxene commonly contains inclusions of olivine and Cr-spinel. Cr-spinel grains in wehrlite are opaque and have two different sizes. Small grains (< 0.2 mm) are anhedral to subhedral and occur as inclusions in clinopyroxene. Large grains (< 0.8 mm) are subhedral and contain fractures filled with magnetite. Magnetite also rims the grains of Cr-spinel. Discontinued veinlets of fine-grained magnetite occur along grain boundaries of clinopyroxene.

Gabbroic Rocks

Gabbroic rocks are well exposed in all four massifs of the BOIC (Fig. 1). Sills and dykes of wehrlite, harzburgite, lherzolite and dunite locally cross cut gabbroic rocks. Gabbroic samples were collected from the BMD massif above the dunite. At BMD, most gabbroic rocks are dominated by plagioclase and clinopyroxene, with minor olivine and Cr-spinel. Plagioclase (up to 70 vol.%) ranges in size from 0.8 to 1.8 mm. Clinopyroxene (20-25 vol.%) has grain sizes from 0.5 to 1.0 mm. Subordinate (up to 5 vol.%). olivine grains are small (0.3-0.8 mm). Discrete grains (0.2-1.2 mm) of orthopyroxene are present in some samples (~1 vol. %). Traces of euhedral Cr-spinel occur as discrete grains or enclosed within plagioclase and clinopyroxene. Chlorite is common as an alteration product of clinopyroxene.

ANALYTICAL PROCEDURES

The concentration of major and minor elements in bulk rocks were determined at the University of Ottawa, using a Philips PW2400 sequential wavelength dispersive XRF. Major elements were obtained from a fused bead made from a mixture of sample (1.5 g) with lithium metaborate (6.0 g) and lithium tetraborate (1.5g) at ˜1050^{o}C. The concentrations of S were determined using a Vista-Pro ICP-OES (University of Ottawa) after digesting samples in *aqua regia* in sealed, screw-top Teflon vials at 150^{o}C.

Platinum group element (PGE) concentrations were determined by isotopic dilution techniques using a mixed spike of ^{101}Ru, ^{105}Pd, ^{190}Os, ^{191}Ir and ^{194}Pt. PGEs were pre-concentrated in a Ni-sulfide bead which was dissolved in 6N HCl, and the filtrate was dissolved in concentrated $HN0_3$. Mass ratios were determined using an Agilent HP 4500 inductively coupled plasma mass spectrometer (ICP-MS; University of Ottawa). Blanks were

0.002-0.007 ng Ir/g flux, 0.002-0.006 ng Os/g flux, 0.07-16 ng Pt/g flux and 0.03-0.9 ng Pd/g flux and 0.002-0.007 ng Ru/g flux. These values are negligible compared to amounts in samples and thus blank corrections were not applied to the results.

Mineral compositions were determined using an automated 4 spectrometer CAMEBAX MBX electron probe (Carleton University) by the wavelength dispersive X-ray analysis method. Counting times were 15 sec per element, except for Fe (20 s) and Ni (40 s). A 15 kV accelerating potential and a 20 nA beam current were applied. The calibration standards used were pure wollastonite (Si, Ca), synthetic spinel (Al), synthetic Cr_2O_3 (Cr), forsterite (Mg), synthetic $MnTiO_3$ (Mn, Ti), pure vanadium metal (V), albite (Na), fayalite (Fe in silicates) and synthetic Fe_3O_2 (Fe in oxides). Fe_2O_3 contents of spinel were determined assuming that stoichiometry is respected.

RESULTS

Mineralogy and Mineral Chemistry

Cr-Spinel

Cr-spinel in harzburgite. Different Cr-spinel grains in individual samples have similar core compositions therefore they are considered primary (Table 1). Values of Cr# (=Cr/[Cr+Al]) range between 0.32 and 0.64 and values of XMg ($Mg/[Mg+Fe^{2+}]$) vary from 0.52 and 0.70. They have low Fe^{3+} ($YFe^{3+} = Fe^{3+}/[Al+Cr+Fe^{3+}]$, < 0.02). Low Cr# samples plot in the field of abyssal peridotites, whilst high Cr# samples plot in the field of forearc mantle peridotites (Fig. 6a). The overall range is similar to that observed by Bédard and Escayola (2010). The TiO_2 contents of Cr-spinel in harzburgite are low, ranging from 0.02 to 0.05 wt%, plotting in the area where subarc and abyssal peridotite fields overlap (Kamenetsky et al., 2001) (Fig. 6b).

Cr-spinel in dunite. In dunite, Cr-spinel cores of different grains in individual samples have also similar compositions, being considered primary (Table 1). The values of Cr# for the cores range between 0.16 and 0.69. The values for XMg range between 0.47 and 0.75. Cr-spinel grains in dunite have higher YFe^{3+} contents (0.03-0.09) than those from harzburgite (< 0.02). Contents of TiO_2 are also higher than those of harzburgite, ranging from 0.04 to 0.78 wt%.

Olivine

The forsterite component of olivine (Fo=100 x Mg/[Mg+Fe]) ranges from 90 to 91 in the analyzed harzburgites, and the contents of NiO from 0.34 to 0.42 % (Table 2). All the harzburgite samples plot within the olivine–spinel mantle array (OSMA) of Arai (1994), which is a restite trend of compositional changes of olivine and Cr-spinel (Fig. 7a). Dunite samples have Fo from 86 to 91. Dunite samples with Fo higher than 90 plot in the OSMA, whereas samples with low Fo (<90) plot outside the OSMA (Fig. 7a). These data suggest that the dunite samples with low Fo components are not in equilibrium with mantle peridotites, and crystallized from more evolved melts that experienced fractional crystallization. Therefore, these more evolved samples were not used for the evaluation of the source mantle for the parental melt.

In dunite the overall NiO contents in olivine range from 0.23 to 0.35 wt% (Table 2). The values of NiO in olivine are slightly lower than those of mantle peridotites (Fig. 7b) and they are not well correlated with Fo contents (Fig. 7b). The data suggests the possible presence of sulfide melt that incorporated Ni. This is consistent with minor, but common occurrences of Ni-rich sulphide minerals in dunite. The evidence suggests the possible presence of sulphide melt during dunite crystallization, but NiO contents in olivine in our

samples are similar to those in the ultramafic cumulate body from the Ni–Cu sulphide deposit in Jinchuan, China (Li et al., 2004).

Nickel contents in olivine coexisting with sulfide melt are controlled by fO_2, fS_2 and temperatures. Brenan (2003) determined the exchange coefficients of Fe and Ni between coexisting olivine and sulfide melt. Sulfide grains in dunites we analyzed contain 26 to 32 wt% Fe and 31 to 41 wt% Ni; with an Fe/Ni weight ratio of 0.78 to 1.1. Considering the extensive oxidation of sulfides to Fe oxides (Fig. 3d), it seems probable that the Ni contents in the original sulfides were probably lower than the measured values. Therefore, we consider that the weight ratios of Fe/Ni in sulfide grains give the maximum values of the original sulfide melt. The weight ratios of Fe/Ni of olivine are 24 to 40. Using these values, the maximum apparent exchange coefficients of Fe and Ni between olivine and sulfide in our dunite samples are evaluated to be ~ 30.8 - 36.3. These values are similar to those observed in S-saturated igneous rocks reported in Brenan (2003), supporting a hypothesis whereby the parental melt for dunite reached S saturation during solidification. This is consistent with the presence of sulfide inclusions in olivine, and textural evidence for the presence of immiscible sulfide melt.

Pyroxene

Orthopyroxene shows XMg (=Mg/Mg+Fe) ranging from 0.91 to 0.92 in harzburgitic rocks. The values of Mg/Fe in orthopyroxene are always higher than Mg/Fe of co-existing olivine in individual samples (Fig. 8). The data are consistent with the equilibration of silicate minerals, as observed in many mantle xenoliths (i.e., Wang et al., 2007). Grain boundaries of pyroxene and olivine are curvilinear, supporting a near-equilibrium relationship. In dunite, orthopyroxene is observed in only one sample, 90365, which was collected near the harzburgite boundary in NAM. The orthopyroxene in this dunite sample forms veinlets and

its composition is not in equilibrium with olivine as XMg (0.91-0.92) are similar to the Fo component (Fo=91) of olivine so we excluded it for the calculation of temperatures and fO_2. Among the minor elements, all samples have low concentrations of TiO_2 in orthopyroxene (< 0.099 wt%). Samples with higher Cr# in spinel have lower concentration of Al_2O_3 in orthopyroxene (Table 3). Samples with Cr#>40 in spinel plot within the field overlapping between abyssal/forearc and the abyssal peridotite field defined by Choi et al. (2008) (Fig. 9).

Clinopyroxene grains were only observed in three samples (TBL-05, 92160 and 92581). The grains show higher XMg (0.934-0.959) than orthopyroxene in individual samples of harzburgite. The compositional relationship between the two pyroxenes is similar to those of mantle xenoliths elsewhere (e.g., Conceição and Green, 2004; Wang et al., 2007), suggesting that the two pyroxenes in our samples are in equilibrium. The equilibrium relationship between clinopyroxene and olivine is also observed where values of XMg show a positive correlation with Fo components of olivine (not shown).

Bulk Rock Major Element Compositions.

Harzburgite bulk rock composition show high concentrations of immobile refractory elements (Table 4), such as Ni (2115-2237 ppm) and Cr (2380-3200 ppm). The composition is similar to typical of residual mantle rocks (Fig. 10). Bulk rock XMg (= atomic ratio of 100*Mg/[Mg + Fe_2O_3 total]) is also high, ranging between 90.6 and 91.5. Calcium and Al contents are low, less than 1.15 wt% CaO and 0.38 to 0.94 wt% Al_2O_3. All dunite samples from the study area have lower concentrations of immobile refractory elements than harzburgite (Table 4): Ni (1830-2920 ppm) and Cr (730-5720 ppm). Bulk rock XMg of dunites range from intermediate to high values (85.5-90.2), and CaO is low (< 1.24 wt%).

Most dunite samples contain low to intermediate concentration of Al_2O_3 (< 2.4 wt%), and low TiO_2 (<0.05 wt%).

Sulfur and Platinum Group Element Concentrations

Sulfur contents in harzburgites range from 24 to 238 ppm with an average of 130 ppm, significantly lower than the primitive mantle value of 250 ppm (McDonough and Sun, 1995). Dunite has higher S contents, with an average of 271 ppm, slightly higher than the primitive mantle value. Individual sample S-contents range from 24 to 894 ppm, however, with the highest concentration of S reflecting higher sulfide mineral modes.

Harzburgites and dunites contain total PGE contents ranging from 18.4 to 44.7 ppb, and 3.65 to 97 ppb, respectively. Harzburgites have high ratios of Ir-type (Ir, Os and Ru) to Pd-type PGEs (Pd, Pt and Rh) (Ir/[Pd+Pt), 0.14 to 0.75 characteristic of a negatively sloped primitive-mantle PGE normalized pattern (Fig. 11a). Iridium-type PGEs remain in the mantle residue during partial melting, as opposed to the relatively incompatible Pd-type PGEs (Pt, Pd and Rh) (e.g., Brenan et al., 2005). In contrast to BOIC harzburgites, dunites have lower ratios of Ir-type/Pd-type PGEs, (Ir/[Pd+Pt) =0.01-0.56), and positively sloped normalized PGE patterns (Fig. 11a). Our data suggests that BOIC harzburgites are restites from mantle melting, whereas the low contents of Ir-type PGEs suggest that dunites are cumulate rocks. This is in accord with the discordant trend of dunite samples relative to OSMA (Fig. 7a)

The values of (Ir/[Pd+Pt]) for both harzburgites and dunites is positively correlated with Fo in olivine (Fig. 11b). The positive correlation between Fo and (Ir/[Pd+Pt]) in BOIC dunite suggests that fractional crystallization resulted in simultaneous decrease of XMg and (Ir/[Pd+Pt]) in the melt. Olivine and minor Cr-spinel are the cumulus minerals in BOIC dunite. Many previous studies have shown that Ir-type PGEs were compatible with these

early crystallizing phases during solidification (e.g., Barnes et al., 1995; Lesher et al., 2001), and this compatible behaviour has been interpreted to have been controlled by olivine (e.g., Barnes and Picard, 1993) and spinel (e.g. Righter et al., 2004) as these minerals may incorporate PGE into their structures. It is also possible that discrete platinum group minerals might have crystallized together with olivine and have been responsible for this trend (see review by Crocket, 2002). The data obtained in this study is consistent with either explanation.

As stated earlier, sulfide was likely present during the solidification of the parental melt for dunite. PGEs have a strong affinity with sulfide melt with their partition coefficients between sulfide melt to silicate melt greater than 1000 (Sattari et al., 2002). In dunite, high concentrations of total PGEs in samples with high concentration of S suggest this possibility. Sulfide melt formed during the crystallization of olivine may have incorporated PGEs.

Estimates of Temperature and Oxygen Fugacity

A positive correlation of XMg values between coexisting minerals suggests chemical equilibrium among the main silicate and oxide minerals, which allows us to calculate equilibrium pressures, temperatures and oxidation conditions of BOIC peridotites. As described in the previous section, minerals in orthopyroxenite and wehrlite veinlets are not in equilibrium with the minerals in host rocks. Therefore, these samples were not used for the calculation.

The two-pyroxene thermometer of Wells (1977) yielded higher temperatures (891^{o}C - 1051^{o}C) than that of Brey and Köhler (1990), which gave temperatures between 930^{o}C and 1033^{o}C. The Ca-in-Opx thermometer (Brey and Köhler, 1990) gave temperatures ranging from 854^{o}C to 1093^{o}C (Table 5). The olivine-spinel Fe–Mg exchange thermometer of Ballhaus et al. (1991) gave systematically lower temperature (681^{o}C to 907^{o}C) presumably

due to subsolidus exchange of Mg and Fe involving spinel at low temperatures (e.g. DeHoog et al. 2004).

Oxygen fugacity is expressed as $\Delta \log fO_2$, which refers to the deviation from the quartz–fayalite–magnetite (QFM) buffer at a specified temperature and pressure. Since our dunite samples do not contain any pressure indicators, and dunite rocks are cross cutting gabbroic rocks, a depth of 8 km was assumed based on typical oceanic crust thickness. A pressure of 0.22 GPa, corresponding to ~ 8 km depth, was used in our calculation both for harzburgite and dunite. Errors due to the uncertainty of pressure are small. Wood et al. (1990) calculated that an error in temperature of 100ºC and in pressure of 1 GPa corresponds to a difference in fO_2 of 0.2 and 0.3 log units, respectively.

The oxygen fugacity was obtained using the equation of Ballhaus et al. (1991), which requires the compositions of spinel and olivine. Although the majority of published oxygen fugacity data uses the olivine–spinel–orthopyroxene equilibria of Nell and Wood (1991) instead of the equation of Ballhaus et al (1991), Parkinson and Arculus (1999) demonstrated that two methods give negligible discrepancy (<0.2 log unit) in the calculated fO_2.

Harzburgites yielded fO_2 values ranging from FMQ -2.37 to FMQ -0.07. The calculated fO_2 values for dunite ranges from FMQ +0.20 to FMQ +1.69. At a given Cr# of Cr-spinel, dunite shows higher oxygen fugacities than harzburgite (Fig. 12).

DISCUSSION

Origin of Harzburgite

Harzburgite in BOIC contains orthopyroxene with low-Al and high XMg; and compositions of olivine and spinel pairs fall in the OSMA (Fig. 7a). Bulk rock compositions of harzburgites are depleted in incompatible elements, and enriched in compatible elements (Fig. 10). Compared to the primitive mantle composition, BOIC harzburgite shows similar

to higher concentrations of Ir-type PGEs (Fig. 11a). The harzburgites contain low S, and do not show a correlation between S and total PGEs (Fig. 13), negating the possibility of a significant role for sulfides in concentrating PGEs in melting residues. During the partial melting, Ir and Os remain in the mantle residue due to their high partition coefficients between mantle minerals and melt (e.g. Righter et al., 2004). Therefore, our PGE data are consistent with a residual mantle origin for BOIC harzburgites, as proposed by Edwards and Malpas (1995); and Batanova et al., (1998).

The contents of Cu and S show a positive correlation and both have lower concentrations than the primitive mantle values of 30 ppm and 250 ppm, respectively (McDonough and Sun, 1995). The low concentrations of these two are consistent with the residual origin for BOIC harzburgite as both Cu and S are incompatible with mantle minerals and preferentially incorporated into a melt during partial melting.

Spatial Distribution of Cr-spinel Cr# in Harzburgite

The Cr# of residual peridotites is to a large extent related to the degree of partial melting because Cr is compatible and Al is incompatible (e.g. Dick and Bullen, 1984; Pagé et al., 2008). Harzburgitic rocks located nearest to the overlying dunite, less than 0.5 km from the contact show high Cr# in Cr-spinel in all massifs; whereas harzburgites sampled further from the contact have lower Cr# (Fig. 14). This relationship implies that harzburgite from shallower levels have undergone high-degrees of partial melting, whereas those from deeper depths have lost less melt. Batanova et al. (1998) also noted that the least depleted mantle rocks in the BOIC occur at the greatest depths.

Origin of Dunite

Dunitic rocks in our samples have several possible origins: ultra-residual mantle, metasomatic products, and cumulates of mafic melts. Highly refractory residual dunite forms

after extensive partial melting (e.g., Griffin et al., 2008). However, BOIC dunites have slightly lower contents of Ni in olivine in comparison with most harzburgites (Fig. 7b). Since Ni concentrations are expected to increase in the residues during partial melting, our data do not support a residual mantle origin for BOIC dunites. Furthermore, the low Ir type PGE concentrations (Fig. 11a) in the dunites are not consistent with a residual origin for BOIC dunites, since these elements remain in the residue during partial melting.

Dunite might also have formed as a metasomatic product of harzburgite through reactions with hydrous mafic melt (e.g., Quick, 1981; Kelemen et al., 1990; Suhr, 1999). The dunites in the BMD massif are voluminous and massive with no fragments of other lithologies in field and hand specimens. The occurrence of the dunite does not appear to support this possibility because dunite bodies formed by metasomatism commonly contain relicts of pre-metasomatic rocks and show reaction zones with harzburgite hosts (e.g. Quick, 1981; Kelemen et al., 1990; Pagé et al., 2008). The thick and massive dunites in BMD cannot plausibly be interpreted in terms of metasomatic transformation of harzburgite, as previously suggested by Suhr et al. (1998). Furthermore, the PGE contents of dunite appear to be not consistent with the metasomatic origin because dunite contains less Ir-type PGEs than harzburgite. Peridotites commonly retain PGE contents and patterns during their metasomatism because mafic melt has low solubility of PGEs, especially Ir-type PGEs, to remove them from peridotites during the metasomatism. For example, orthopyroxenite formed from harzburigite by metasomatism contain essentially identical PGE contents as the precursor harzburgite (Wang et al., 2008).

The low Ir-type PGE concentrations and low ratios of Ir-type PGE to Pd-type PGE (Fig. 11a) in the BOIC dunites are most consistent with a cumulate origin since partial melting in the mantle produce low concentration of Ir-type PGE in derivative melts. The

proposed interpretation is further supported by the variations in Fo components in BOIC olivine. For example, olivine from mantle residues typically has the values between Fo88 and Fo93 (Fig. 7) whereas BOIC dunites have Fo between 86 and 90. Therefore, we consider that the dunites in the BOIC are cumulates of a melt. This is further supported by layers of layering in dunite including Cr-spinel-rich bands observed in dunites from Blow-Me-Down (Fig. 5).

Oxidation Condition of the Mantle

All BOIC harzburgites show fO_2 below the FMQ buffer. The oxidation state of the asthenospheric mantle is considered to be below the FMQ buffer as indicated by the data from abyssal peridotites, FMQ -0.9 (Bryndzia and Wood, 1990) and mantle peridotites in continental rifts that have been affected by asthenosphere derived melts (Ionov and Wood, 1992). On the other hand, magmas and mantle peridotites in subduction zones commonly show higher fO_2 values than the FMQ buffer (Parkinson and Arculus, 1999). The high fO_2 values in subduction zone environments are commonly explained by the ingress of oxidized fluids or melts derived from dehydrating subducting plates (Parkinson and Arculus, 1999). The calculated fO_2 values of the majority of BOIC dunites are higher than the FMQ buffer; and we suggest that this high fO_2 is related to the subduction origin of the melts from which BOIC dunites formed. Dunite samples with low Fo components (<90) show similar fO_2 values of samples with Fo higher than 90 indicating that fractional crystallization did not change fO_2 values.

Possible Tectonic Setting

Our data, as well as previous data, reveal a wide range in Cr# for Cr-spinel in BOIC harzburgites. The variation is large even within each massif and the data plot across the abyssal peridotite / forearc mantle fields (Fig. 6a). Cr-spinel in dunite from the BOIC also

shows a large variation in Cr#. The Cr# of high Mg-dunites where Fo components of olivine are greater than 90, also show a wide range (Fig. 7a). Since these samples plot in the olivine-spinel mantle array of Arai (1994), the Cr# should be similar to the Cr# of the primitive melt or in equilibrium with the source mantle peridotites. Therefore, we suggest that the observed large variation in Cr# in Cr-spinel in dunite reflects the Cr# of the source mantle from which these melts were derived. Dunites with low Cr spinel were formed from melts extracted from low-Cr# mantle, whereas dunites with high Cr spinel record the melting of high-Cr# mantle.

Cr-spinel from abyssal peridotites has Cr# values below 0.55 (Dick and Bullen, 1984). Cr-spinel in forearc mantle peridotites contains high Cr#, most commonly over 0.45 (Arai, 1994 and Parkinson and Pierce, 1998). Cr-spinel with Cr# ranging between 0.4 and 0.55 is found in refractory abyssal peridotite formed at fast spreading ridges or relatively fertile forearc peridotite (Fig. 6a).

Refractory abyssal peridotites form at ridges with fast spreading rates, such as the East Pacific Rise (e.g., Niu and Hekinian, 1997). On the other hand, abyssal peridotites formed at slow spreading ridges, such as the Atlantic Ocean lithosphere and proto Caribbean oceanic lithosphere are less refractory containing Cr-spinel with low Cr#, < 0.4 (Michael and Bonatti, 1985; Saumur et al., 2010). The Cr-spinel with low Cr# in our harzburgite shows characteristics of an abyssal peridotites most likely formed in a slow spreading ridge, evidence further supported by the minor elements from orthopyroxene grains in these rocks (Fig. 9).

On the other hand, harzburgite with high Cr# > 0.4 Cr-spinel (Fig. 6a) more likely formed during extensive partial melting in a subduction setting. The proposed interpretation is reinforced by the observed higher fO_2 values of BOIC dunites (Fig. 12). The Cr# of Cr-spinel in BOIC harzburgites are lower than those of some forearc mantle peridotites, such as

the Marianas (up to 0.82; Ishii et al., 1992; Fig. 6a) and the western Himalayas (0.76-0.83; Hattori and Guillot, 2007), but are similar to those of the forearc mantle peridotites from the Dominican Republic (Saumur et al., 2010) and Thetford Mines ophiolite (Pagé et al., 2008).

It is likely that the development of large volumes of highly refractory mantle peridotites requires a geologically long period. Highly refractory mantle peridotites are reported in the Marianas and western Himalayas. Subduction has been in operation for more than 50 Ma in the Marianas (Ishizuka et al., 2011) and over 160 Ma in the western Himalayas (Van der Voo et al., 1999). In contrast, the mantle below the northern Dominican Republic is not highly refractory where the subduction was short-lived from the very late Cretaceous to the mid Eocene (Saumur et al., 2010). The subduction related to the Thetford Mines ophiolite was also short-lived because it was obducted very quickly after its formation (Tremblay et al., 2011). At BOIC, radiometric age data suggest a small age difference of about 15 Ma between the seafloor-spreading formation of the BOIC tholeiitic crust (ca 484 Ma, Jenner et al., 1991) and obduction (metamorphic sole 469 Ma, Dallmeyer and Williams, 1975). Since obduction in BOIC happened as a result of subduction (Cawood and Suhr, 1992), the time span of 15 Ma is the maximum estimate for the duration of subduction recorded by BOIC.

The proposed interpretation based on dunite chemistry is supported by the boninitic geochemical signature of pyroxenite veins in the harzburgite unit (Varfalvy et al., 1997); and by trace element inversions applied to BOIC dunitic and orthopyroxenitic crustal cumulates (Bédard 2007). Boninitic magmas are commonly associated with the infant stages of subduction (e.g. Whattam and Stern, 2011; Ishizuka et al., 2011. Therefore, we infer that the boninites from the BOIC were formed during the initial stage of subduction, but this event did not last long enough to produce highly refractory peridotites in the mantle wedge.

Comparison with Previous Models

Various opinions have been proposed for the origins of the BOIC. They range from oceanic lithosphere formed at a normal mid-oceanic ridge to its formation in arc setting. The 'normal' ridge lithosphere origin is primarily based on the major element chemical compositions of diabase dikes, basalts and gabbros in the BOIC which are similar to those of modern mid-oceanic ridge igneous rocks (e.g., Suen et al., 1979; Casey et al., 1985).

A supra-subduction setting for BOIC gabbroic rocks was proposed by several authors in 1991. A boninitic affinity was proposed for the ultramafic cumulates at NAM by Bédard (1991), based on the low Ti contents of pyroxenes, high Cr# of Cr-spinel, and abundance of orthopyroxene. It was proposed that the boninitic melts intruded pre-existing gabbroic rocks (Bédard and Hébert, 1996). Elthon (1991) suggested a supra-subduction zone setting for the BOIC based on low concentrations of high-field strength elements of dioritic and basaltic rocks from NAM. Jenner et al., (1991) interpreted the Little Port complex in the Coastal Complex as part of an arc, and named the BOIC as a supra-subduction-zone ophiolite.

Cawood and Suhr (1992), and Suhr and Cawood (2001) based on geochemical and structural field evidence from the Lewis Hills massif proposed that the BOIC formed as a spreading ridge that intersected an old arc lithosphere of the Coastal Complex along a ridge-transform fault. This model was refined by Kurth et al. (1998, 2004).

Our study shows that the geochemical signatures of harzburgites cannot be explained by one tectonic setting, oceanic ridge or subduction zone. Harzburgite shows geochemical characteristics of both abyssal and forearc peridotites, the latter formed during extensive partial melting for the parental melt of dunite within 0.5 km from dunite contact.

Abyssal peridotite and MORB-type basalt occurring with forearc peridotites were described in the Coast Range ophiolite in California by Shervais (2001) and Choi et al.,

(2008). Choi et al., (2008) suggested the formation of the Coast Range ophiolite in subduction setting based on the geochemistry of Cr-spinel and trace and minor element abundance of pyroxenes, but the Coast Range ophiolite locally contains domains of abyssal peridotite. They interpreted the block of abyssal peridotites as a relict prior to hydrous melting in the mantle wedge. Although the geochemistry of Cr-spinel and pyroxene in our BOIC samples are similar to that of the Coast Range ophiolite in California, abyssal-type peridotites are predominant in the harzburgitic unit in the BOIC and it is difficult to explain as a local relict in the BOIC.

Another possible tectonic setting to produce geochemical signatures of abyssal and subduction is a back arc where arc lithosphere experiences a local rift to produce MORB-like magmas. Cawood and Suhr (1992) suggested that seafloor spreading possibly in the back arc of a mature arc system produced gabbroic rocks and sheeted dykes, where highly refractory mantle changed to less-depleted oceanic mantle. This seafloor spreading could have been caused by pericollisional extension. The term pericollisional was first described by Harris (1992) to explain opening of small basins in subduction zone that may be obducted during or shortly after they form by progressive convergence. Van Staal (2007); Zagorevski and van Staal (2011) suggested pericollisional spreading that formed due to rollback of the downgoing slab into a reentrant in the Laurentian margin to explain the origin the BIOC and the southern extension of the ophiolites in Quebec, such as Mont Albert and the Thetford Mines complexes.

The time sequence from supra-subduction to oceanic setting appears not consistent with the correlation in harzburgites between Cr # of Cr-spinel and distance from dunite observed in this study (Fig. 11). Our geochemical data suggest oceanic conditions changed to subduction setting before the dunite formation. The field evidence for the intrusion of

dunite to gabbroic rocks and harzburgites also suggest the subduction setting followed the oceanic conditions. Furthermore, if the environments changed from supra-subduction to ridge setting, the parental melt for the voluminous gabbroic rocks and sheeted dykes had to pass through the mantle peridotites. The mantle peridotites should have been extensively metasomatized by the melt. The lack of such metasomatism and the distribution of Cr# of Cr-spinel in relation to the dunite unit suggest that the environments changed from oceanic to supra-subduction setting during the BOIC development possible. We therefore conclude that the dunite is a product of subduction initiation and this resulted in the change in harzburgites from abyssal peridotite to a refractory forearc-type peridotites.

CONCLUSIONS

Bulk rock chemistry, mineral chemical data and calculated fO_2 values we have obtained indicate (as proposed previously) that BOIC harzburgites are refractory mantle residues after partial melting. In contrast, the PGE abundance profiles in all dunite samples show a cumulate signature with low Ir-type PGEs and low ratios of Ir-type to Pd-type PGEs. The dunite signature is distinctly different from that of the residual mantle peridotites. Furthermore, dunites do not fall along the olivine-spinel mantle array, have variable but high spinel Cr#, and have higher fO_2 than associated harzburgitic peridotites; none of which are compatible with an origin as ultra-depleted mantle restites. Consequently, we suggest a cumulate origin for most BOIC dunites. Massive dunitic cumulate rocks from BMD are up to 3 km. These data and spatial relationships suggest that the BMD massif was closest to the zone of upwelling, that these melts underplated gabbroic, rocks and spread laterally towards the north. This explain why much of the mantle peridotites in TBL and NAM massifs retain

geochemical signatures of abyssal peridotites and have escaped overprints of further depletion during the subduction.

The BOIC is interpreted as the vestiges of an ephemeral, peri-continental oceanic lithosphere which formed at a slow spreading ridge. The harzburgites of the BOIC show obvious subduction signatures. Moderate Cr# values of spinel and the overall geochemically signature of BOIC harzburgites record melt extraction beneath the spreading ridge, whereas high Cr# values in Cr-spinel likely formed in subduction settings. The generally higher Cr# of spinel in BOIC dunites suggests that the source mantle for its parental melt was refractory, similar to forearc mantle, indicating progressive depletion in the mantle during the evolution of the BOIC. Therefore the compositional variation of Cr-spinel reflects a change in the tectonic settings during BOIC formation and a progressive depletion in the mantle through melt extraction in a subduction setting.

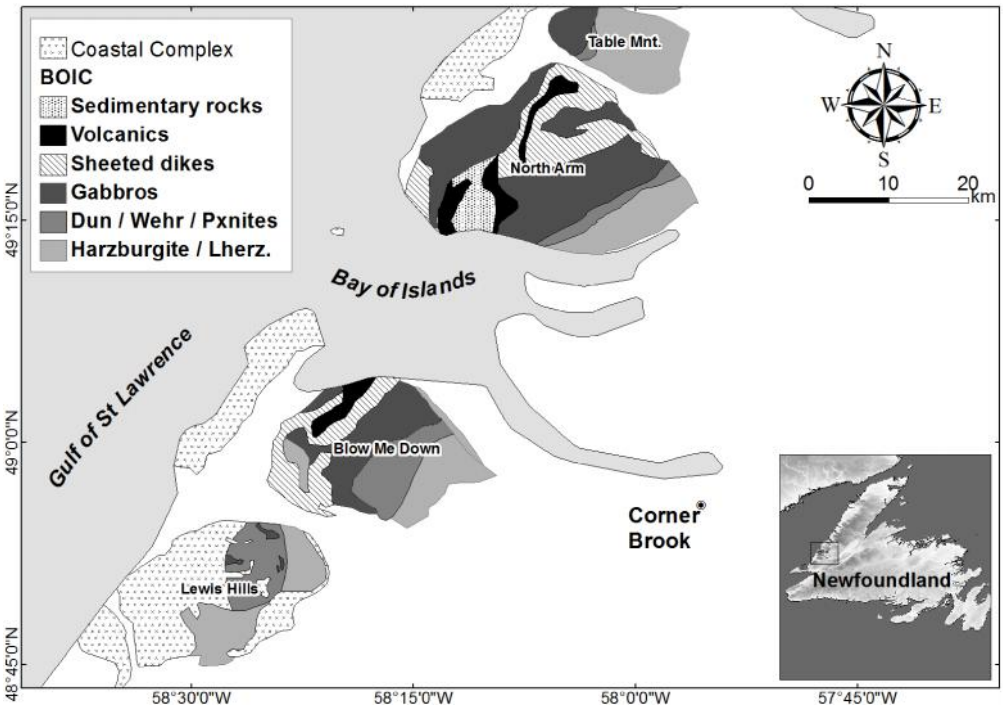

Figure 1: Location map of the study area in insert and simplified geological map of the Bay of Islands Ophiolitic Complex. City of Corner Brook is shown with double circle. Modified after Suhr (1992).

Figure 2: Dike of dunite cutting the harzburgite unit in Table Mountain.

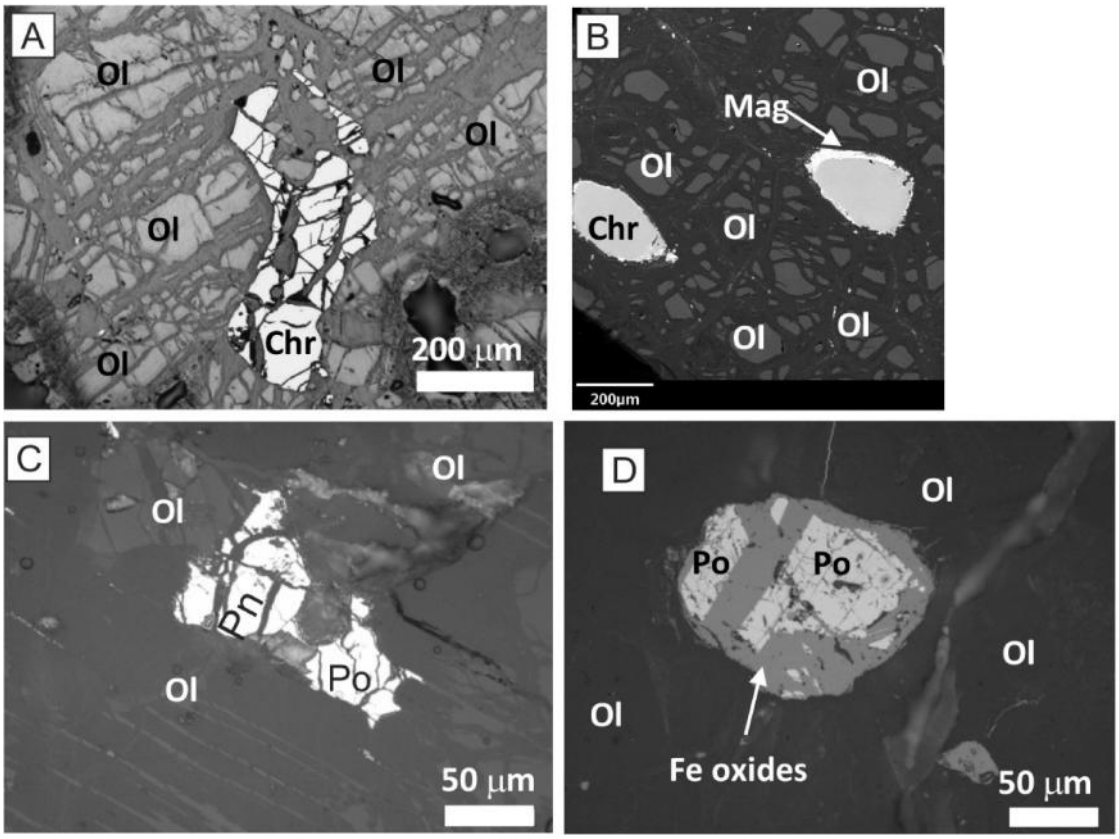

Figure 3: BOIC rocks. (A) Photomicrograph of harzburgite, sample 8964 from NAM, under plain reflected light, showing a Cr-spinel grain (Chr) and olivine (Ol). (B) Back-scattered electron image of Cr-spinel (Chr) rimmed by magnetite (Mag) in dunite, sample 8928, from NAM. (C) Photomicrograph of angular pyrrhotite (Po) and pentlandite (lighter yellow, Pn) surrounded by olivine (Ol) grains in harzburgite, sample 92160, from NAM under plain reflected light. (D) Photomicrograph of pyrrhotite (Po) altered to Fe oxide (gray) in dunite, sample 92111, from NAM under plain reflected light.

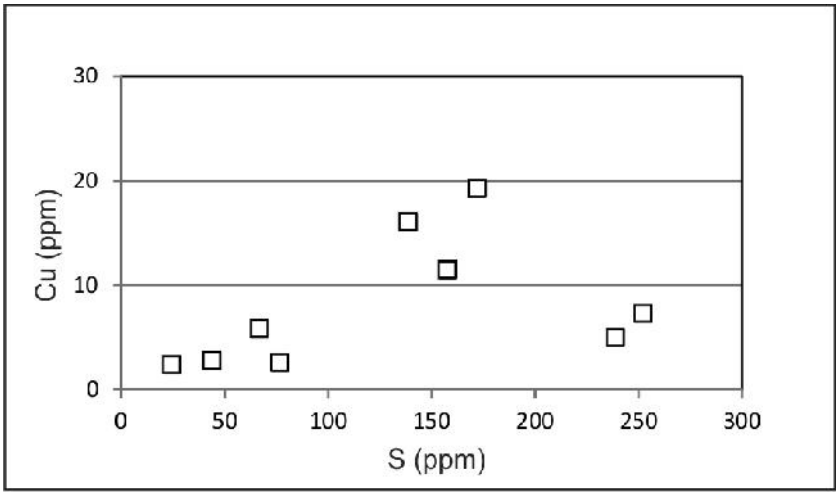

Figure 4: Plot of Cu (ppm) vs S (ppm) in harzburgite BOIC.

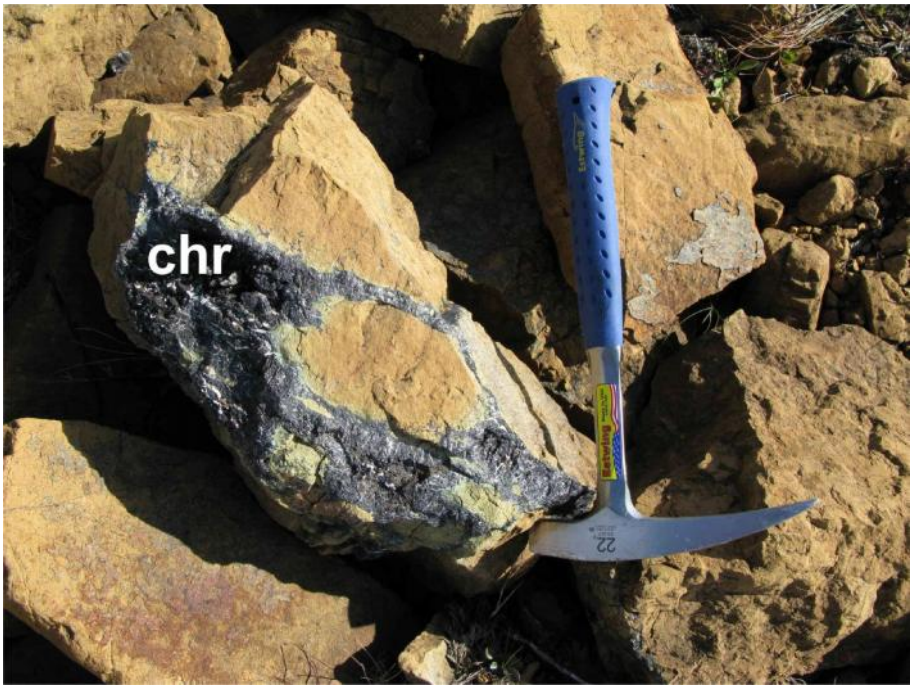

Figure 5: Cr-spinel-rich bands (chr) in dunite from BOIC.

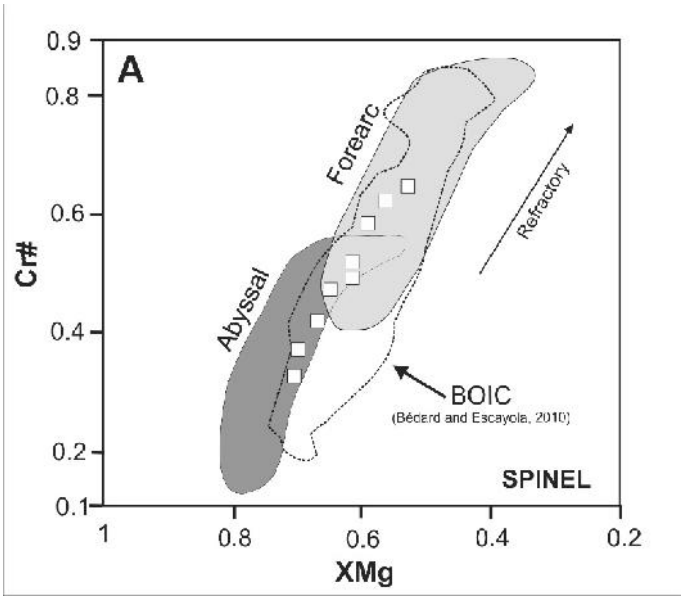

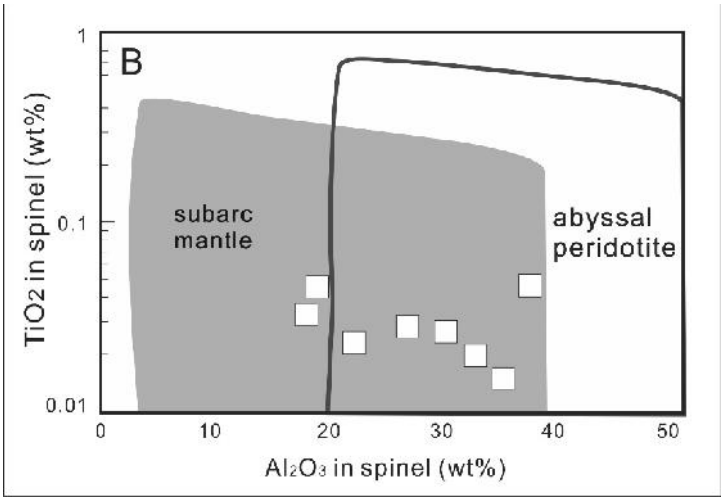

Figure 6: The composition of Cr-spinel cores from harzburgites. Each point represents the average composition of the grains in one sample. (A) Plot of Cr# vs XMg of Cr-spinel. Dark grey field is for abyssal peridotite (Dick and Bullen, 1984); light grey field is for peridotite mantle forearc is defined by Cr-spinel data from serpentinized peridotites exhumed in the Mariana forearc (Ishii et al., 1992) and dashed line shows the compilation of the data from the BOIC (Bédard and Escayola, 2010). The arrow shows the compositional change of Cr-spinel in residual mantle peridotites during partial melting. (B) TiO_2 vs Al_2O_3 in Cr-spinels. Fields for Subarc mantle and abyssal peridotites are from Kamenetsky et al. (2001).

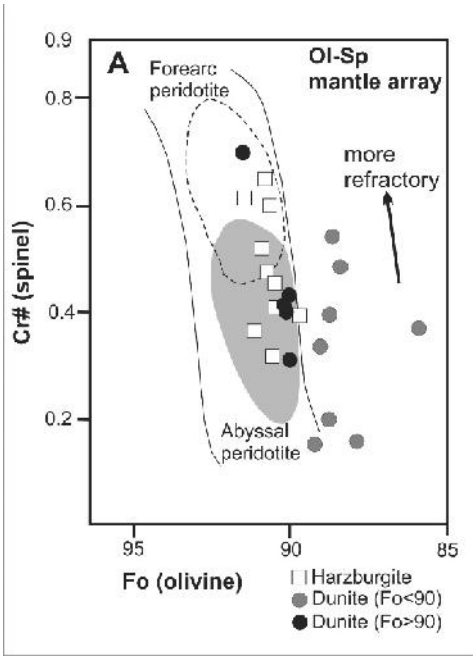

Figure 7a: Forsterite (Fo) component of olivine vs Cr# [Cr/(Cr+Al)] of Cr-spinel in harzburgite and dunite. Each point represents the average composition of the cores of Cr-spinel in one sample. Compositional range of mantle peridotites (Ol-Sp mantle array) is from Arai (1994).

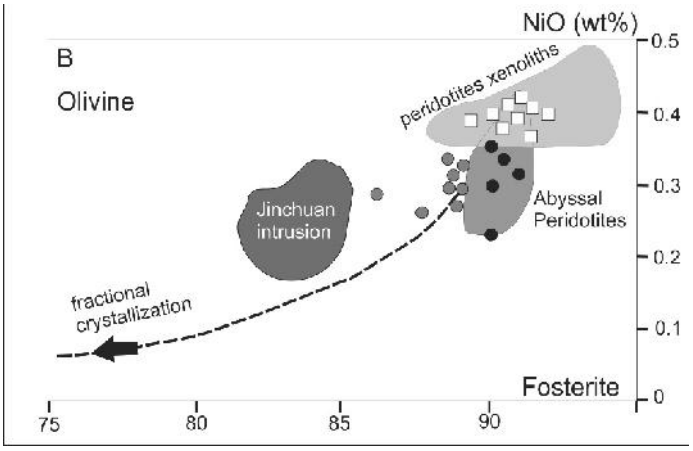

Figure 7b: Contents of NiO and forsterite components in olivine from harzburgite and dunite. The dashed line and the arrow show the compositional variation of olivine during fractional crystallization (Sato, 1977). Light grey field is for peridotites xenolith in kimberlites (Sato 1977), medium grey field for abyssal peridotites are from Hattori et al. (2010) and dark grey field is for ultramafic rocks from the Jinchuan intrusion, Ni–Cu sulfide deposit, western China (Li et al., 2004).

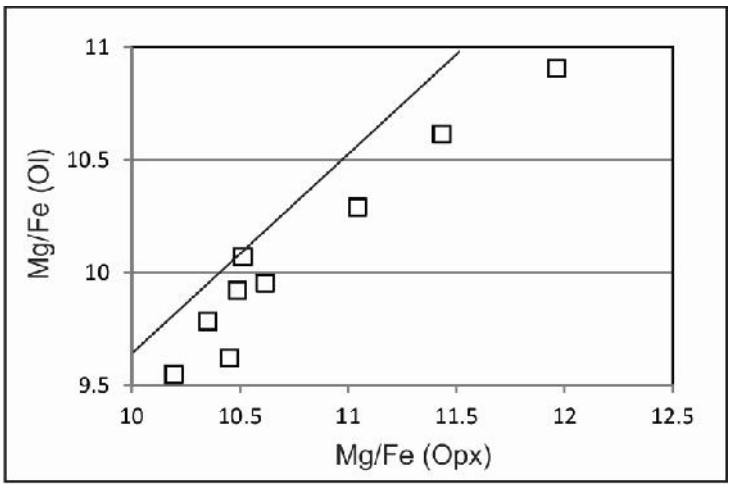

Figure 8: Plot of Mg/Fe of olivine vs Mg/Fe of orthopyroxene in harzburgite BOIC. The equilibrium line is from Peters (1968).

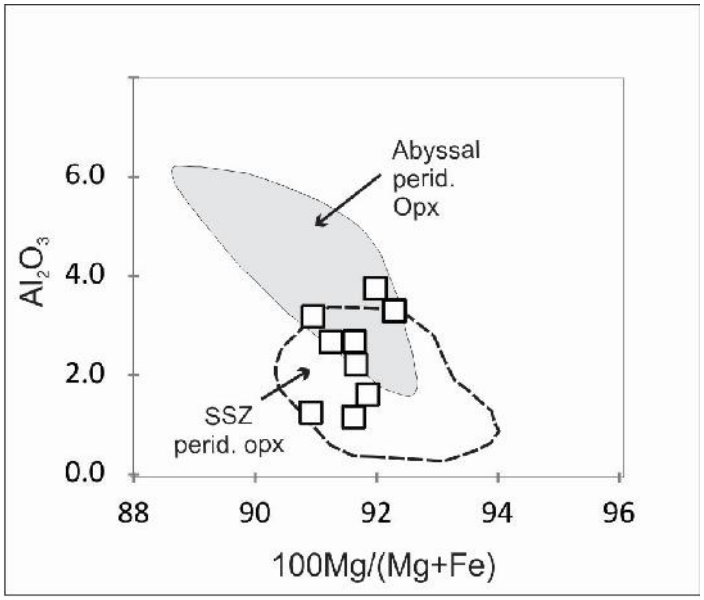

Figure 9: Plot of pyroxene minor element in harzburgite: XMg versus Al_2O_3 in px. Fields for abyssal peridotites shaded and for SSZ peridotite pyroxenes shown as dashed lines (Choi et al., 2008).

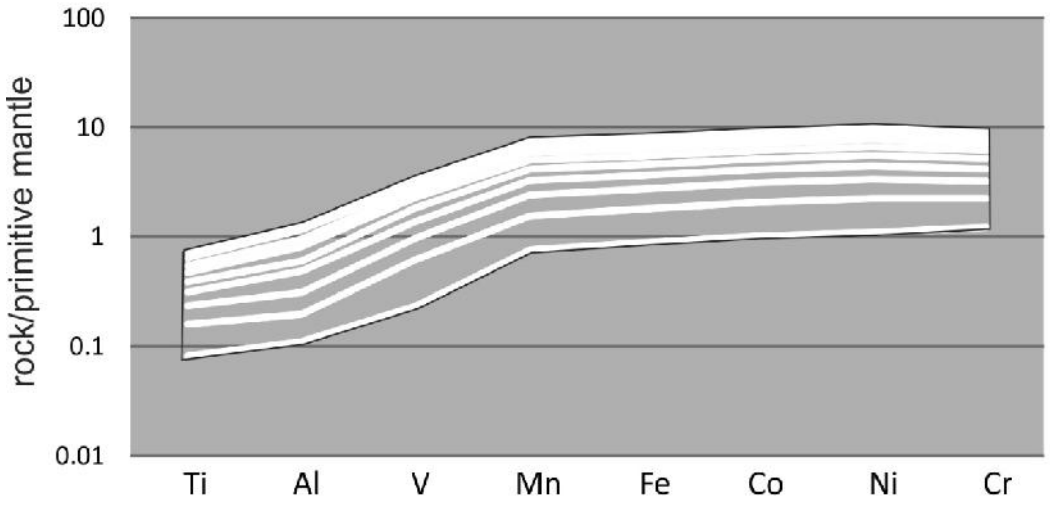

Figure 10: primitive-mantle normalized values of bulk rock minor elements of harzburgite. Primitive mantle values are from McDonough and Sun (1995).

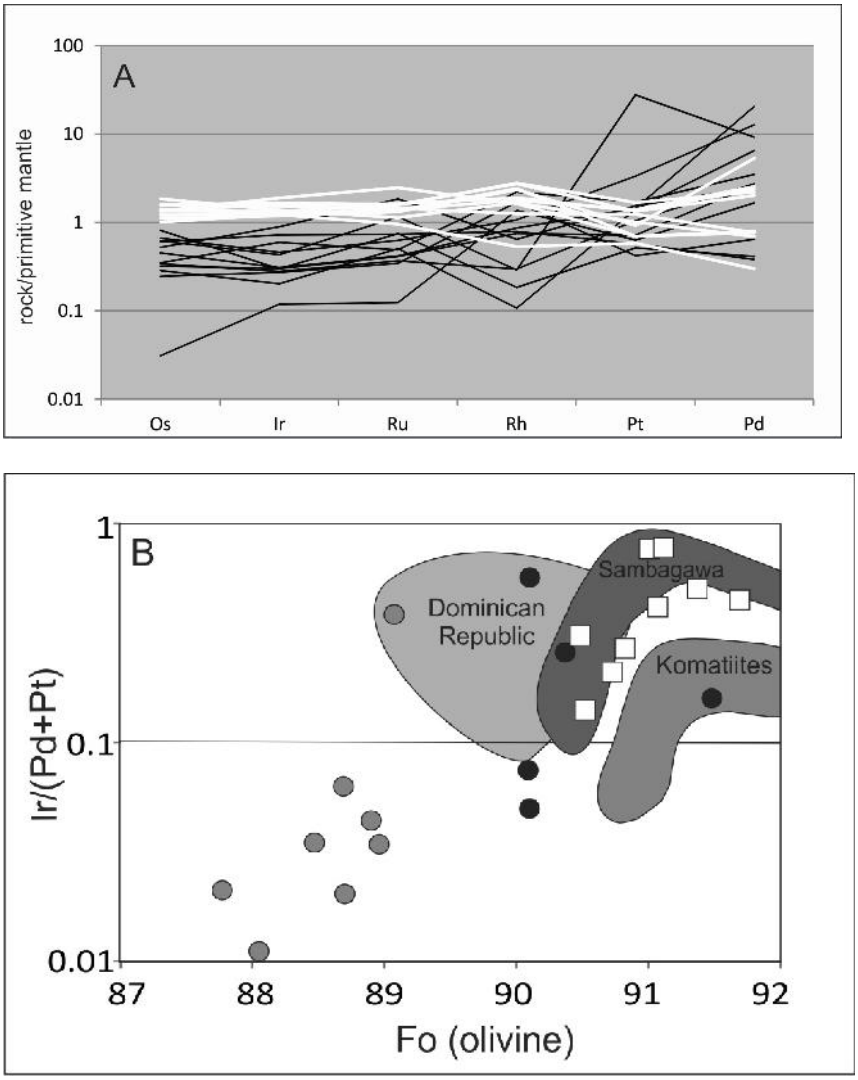

Figure 11: (A) primitive-mantle normalized values of PGE for harzburgite (white lines, n = 9) and dunite (black lines, n = 13)," n" is the number of samples. Primitive mantle values are from McDonough and Sun (1995). (B) Weight ratio of Ir/(Pd+Pt) in bulk rocks versus Fo components in olivine from samples from the BOI. Symbols are the same as Fig. 7. Data for serpentinites from Dominican Republic are from Saumur et al. (2010), for Sambagawa peridotites from Hattori et al. (2010) and komatiites from Puchtel et al. (2004).

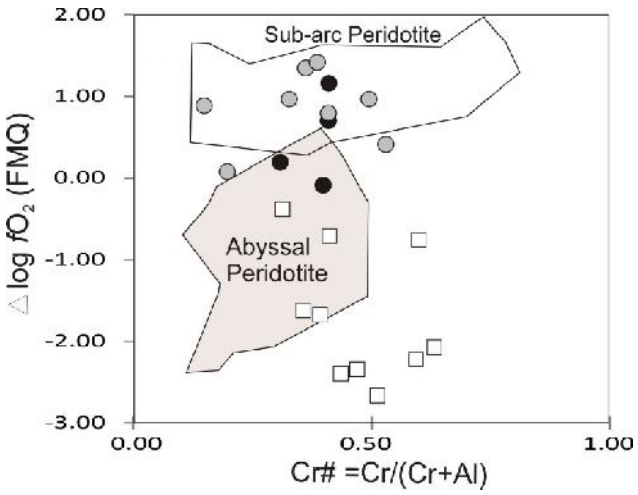

Figure 12: Plot of $\triangle \log fO_2$ (FMQ) *vs* Cr# of Cr-spinel. Symbols are the same as Fig. 7. Data sources: light grey field is for abyssal peridotites (Bryndzia and Wood, 1990), Subarc mantle field include those from Ichinomegata in Japan (Wood and Virgo, 1989), Grenada in Lesser Antilles arc (Parkinson et al., 2003), Avacha, Kamtchatka (Arai et al., 2003) and Marelava in Vanuatu arc, Santa Isabel and San Jorge in Solomon islands and the Simcoe area in Cascade arc (Parkinson and Arculus, 1999). Dark grey field is for mantle harzburgites from Thetford Mines Ophiolite Complex (Pagé et al., 2008).

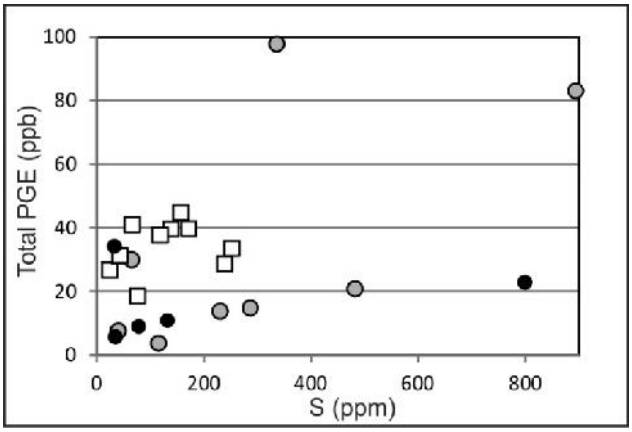

Figure 13: Plot of total PGE *vs* sulphur in harzburgite and dunite from BOIC. Symbols are the same as Fig. 7. Note that the total PGE contents of dunite are broadly correlated with S contents.

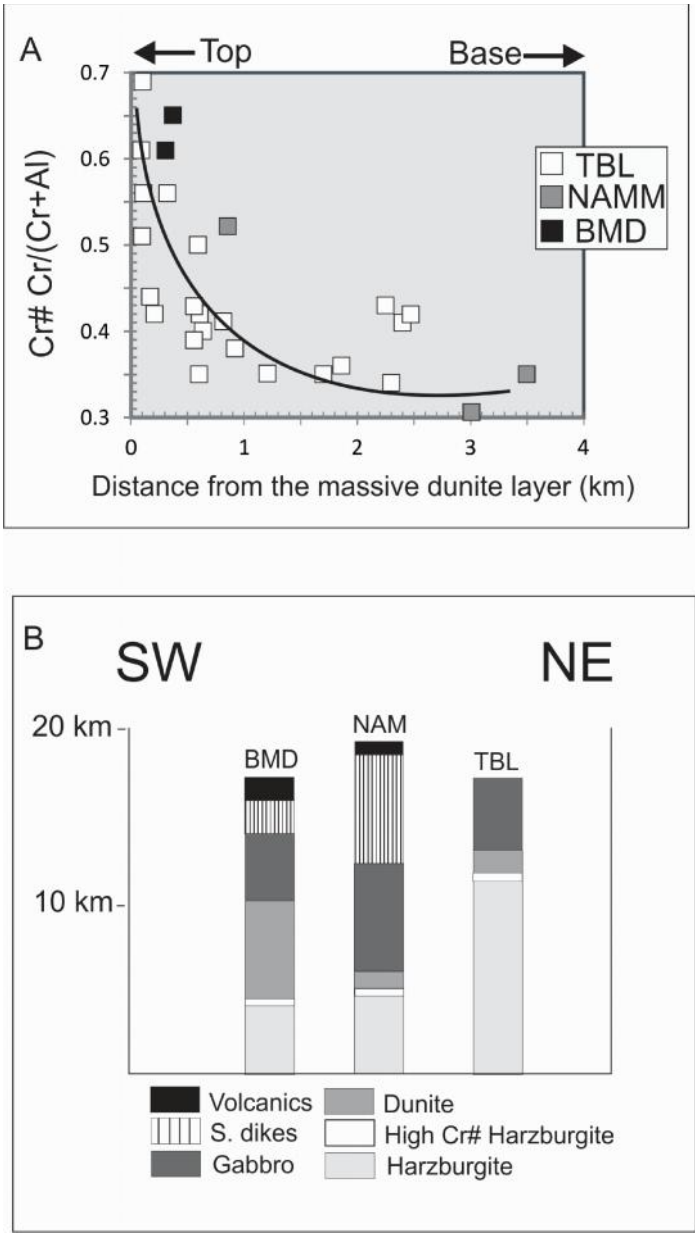

Figure 14: (A) Cr# in the harzburgite samples from BOIC versus the distance from the massive dunite layer contact. The distance to the overlying dunite is the minimum distance on the surface as it was obtained from the map. Although the apparent thickness of harzburgite in TBL massif is greater than 7 km, the diagram shows the distance up to 4 km because there are abundant sills and dikes of dunite at distances between 4 and 8 km. Harzburgite in these areas show high Cr# (0.5- 0.75). The evidence suggests the local derivation of partial melt to form dunite. Data from TBL include those obtained in this study and from Suhr and Robinson (1994). (B) Stratigraphic section of the BOIC massifs showing the spatial correlation between the Cr# in harzburgite and the massive dunite layer contact.

TABLE 1: COMPOSITONS OF REPRESENTATIVE SPINEL GRAINS FROM BAY OF ISLAND OPHIOLITIC COMPLEX

Location	Blow-Me-Down									Table Moutain				North Arm								
Sample	BMD-11	BMD-12	BMD-13	BMD-15	BMD-17	BMD-18	BMD-19	BMD-22	BMD-23	TBL-01	TBL-03	TBL-04	TBL-05	8863	8928	89405	92111	92116	90365	8964	92160	92581
Rock[1]	Dun	Dun	Dun	Dun	Dun	Dun	Dun	Hz	Hz	Hz	Hz	Hz	Hz	Dun	Dun	Dun	Dun	Dun	Dun	Hz	Hz	Hz
SiO_2	0.02	0.03	0.06	0.01	0.05	0.03	0.07	0.05	bdl	0.01	0.02	0.03	0.04	bdl	0.03	0.11	bdl	0.01	0.03	0.00	bdl	bdl
TiO_2	0.17	0.41	0.33	0.08	0.09	0.24	0.48	0.03	0.03	0.03	0.01	0.02	0.02	0.31	0.05	0.19	0.78	0.14	0.20	0.03	0.05	0.02
Al_2O_3	49.87	33.59	31.47	35.98	48.38	50.85	31.56	20.51	18.63	29.80	29.66	22.59	34.56	26.64	31.63	22.42	31.74	37.96	15.80	26.11	37.91	40.48
Cr_2O_3	14.84	32.69	34.74	28.55	17.10	14.74	30.15	47.65	50.17	39.83	40.04	47.04	33.93	36.36	32.75	41.45	27.21	27.64	51.31	42.87	31.58	28.57
V_2O_3	0.19	bdl	0.21	0.16	bdl	0.14	bdl	bdl	bdl	bdl	bdl	bdl	bdl	bdl	bdl	bdl	bdl	bdl	bdl	bdl	bdl	bdl
FeO	18.26	16.81	19.55	19.96	15.35	16.00	23.56	18.02	18.60	14.52	15.41	17.36	14.79	22.30	21.00	23.48	28.55	16.70	21.48	15.93	13.76	15.84
MnO	0.04	0.24	0.05	0.05	0.12	0.04	0.22	0.23	0.25	0.20	0.21	0.23	0.19	0.36	0.18	0.25	0.26	0.16	0.33	0.21	0.13	0.15
MgO	17.67	15.04	14.74	15.47	17.49	19.11	13.11	12.08	10.85	14.20	14.04	12.27	15.15	13.69	13.49	10.36	10.52	16.39	9.92	13.40	16.43	16.27
CaO	0.01	bdl	bdl	0.01	0.02	0.01	bdl	0.01	bdl	0.02	0.02	0.01	0.01	bdl	0.00	0.00	bdl	bdl	0.00	bdl	bdl	bdl
ZnO	0.07	bdl	0.10	0.12	bdl	0.08	bdl	bdl	bdl	bdl	bdl	bdl	bdl	bdl	bdl	bdl	bdl	bdl	bdl	0.02	bdl	bdl
TOTAL	101.1	98.8	101.2	100.4	98.6	101.2	99.2	98.6	98.5	98.6	99.4	99.5	99.1	99.7	99.1	98.3	99.1	99.0	99.1	98.6	100.0	101.3
YFe^{3+}[2]	0.054	0.032	0.053	0.069	0.032	0.051	0.081	0.023	0.011	0.001	0.006	0.011	0.013	0.089	0.060	0.055	0.094	0.048	0.034	0.011	0.012	0.013
XMg[3]	0.70	0.65	0.63	0.66	0.71	0.75	0.58	0.57	0.52	0.64	0.63	0.57	0.66	0.62	0.60	0.49	0.47	0.70	0.48	0.61	0.70	0.68
Cr#[4]	0.17	0.39	0.43	0.35	0.19	0.16	0.39	0.61	0.64	0.47	0.48	0.58	0.40	0.48	0.41	0.55	0.37	0.33	0.69	0.52	0.36	0.32

(1): Dun = dunite, Hz = harzburgite

(2): $YFe^{3+} = Fe^{3+}/(Al+Cr+Fe^{3+})$

(3): $XMg = Mg/(Fe^{2+}+Mg)$

(4): Cr#=100 Cr/(Cr+Al)

bdl = below detection limit

TABLE 2: COMPOSITONS OF REPRESENTATIVE OLIVINE GRAINS FROM BAY OF ISLAND OPHIOLITIC COMPLEX

Location	Blow-Me-Down									Table Moutain				North Arm								
Sample	BMD-11	BMD-12	BMD-13	BMD-15	BMD-17	BMD-18	BMD-19	BMD-22	BMD-23	TBL-01	TBL-03	TBL-04	TBL-05	8863	8928	89405	92111	92116	90365	8964	92160	92581
Rock[1]	Dun	Dun	Dun	Dun	Dun	Dun	Dun	Hz	Hz	Hz	Hz	Hz	Hz	Dun	Dun	Dun	Dun	Dun	Dun	Hz	Hz	Hz
SiO_2	40.74	40.60	40.96	40.83	40.48	41.02	40.52	40.92	40.92	41.09	41.44	41.41	41.11	40.04	40.95	40.42	39.92	39.98	40.63	41.07	41.82	40.09
TiO_2	0.0066	0.0167	0.0050	0.0259	0.0050	bdl	bdl	bdl	bdl	bdl	0.0017	0.0517	bdl	bdl	0.0033	0.0033	0.0100	bdl	bdl	bdl	bdl	bdl
Al_2O_3	0.01	0.01	0.01	0.01	0.00	0.01	bdl	bdl	0.01	0.01	0.02	bdl	bdl	bdl	0.01	bdl	0.02	0.02	0.01	0.02	bdl	bdl
Cr_2O_3	bdl	0.00	0.00	bdl	bdl	bdl	bdl	bdl	bdl	bdl	bdl	bdl	bdl	bdl	bdl	0.02	0.05	bdl	0.01	bdl	bdl	bdl
FeO	11.94	9.14	9.51	10.73	10.84	10.37	10.59	8.30	8.80	8.91	9.11	8.87	9.17	10.76	9.65	10.78	13.42	9.43	9.40	8.47	8.52	8.89
MnO	0.14	0.18	0.16	0.26	0.15	0.11	0.19	0.17	0.12	0.13	0.12	0.12	0.13	0.19	0.19	0.16	0.22	0.15	0.16	0.15	0.11	0.16
MgO	48.65	48.89	50.23	49.36	48.27	49.41	47.70	49.41	49.51	49.27	49.41	49.34	49.59	47.69	49.16	47.68	45.38	48.25	49.57	49.55	50.70	48.87
NiO	0.27	0.32	0.29	0.30	0.29	0.30	0.34	0.40	0.39	0.39	0.40	0.38	0.42	0.34	0.23	0.35	0.28	0.33	0.31	0.39	0.34	bdl
CaO	0.11	0.11	0.13	0.13	0.14	0.11	0.10	0.01	0.04	0.01	0.02	0.03	0.03	0.05	0.08	0.05	0.05	0.06	0.03	0.01	bdl	bdl
TOTAL	101.9	99.3	101.3	101.6	100.2	101.3	99.4	99.2	99.8	99.8	100.5	100.2	100.4	99.1	100.3	99.5	99.4	98.2	100.1	99.7	101.5	98.0
Fo[2]	88	90	90	89	89	89	89	91	91	91	91	91	90	89	90	89	86	90	91	91	91	91

(1): Dun = dunite, Hz = harzburgite

(2): Fo=100 Mg/(Mg+Fe).

bdl = below detection limit

TABLE 3: COMPOSITONS OF REPRESENTATIVE PYROXENE GRAINS FROM BAY OF ISLAND OPHIOLITIC COMPLEX

Location	Othopyroxene									Clinopyroxene		
Sample	BMD-22	BMD-23	TBL-01	TBL-03	TBL-04	TBL-05	8964	92160	92581	TBL-05	92160	92581
Rock(1)	Hz	Hz	Hz	Hz	Hz	Hz	Hz	Hz	Hz	Hz	Hz	Hz
SiO2	57.0	57.9	55.9	56.5	56.6	56.7	57.0	55.4	55.1	53.5	51.6	52.2
TiO2	0.0017	0.005	0.012	0.007	0.003	0.013	0.018	0.005	0.01	0.01	0.10	0.09
Al2O3	1.51	1.06	2.59	2.58	1.14	2.89	2.22	3.22	3.77	2.77	3.98	4.01
Cr2O3	0.56	0.32	0.81	0.82	0.37	0.84	0.68	0.72	0.89	0.95	1.19	1.24
FeO	5.43	5.60	5.54	5.67	6.07	5.92	5.42	5.50	5.23	2.02	2.08	1.99
MnO	0.17	0.13	0.16	0.14	0.17	0.14	0.16	0.15	0.14	0.06	0.09	0.05
MgO	34.2	34.2	33.2	33.0	33.9	33.1	33.6	33.9	33.6	16.9	16.6	16.4
CaO	0.78	0.57	1.53	1.39	0.43	0.93	1.32	0.61	0.58	24.2	23.1	24.0
Na2O	bdl	0.004	0.01	0.01	0.02	0.00	0.00	0.00	0.00	0.04	0.28	0.16
K2O	bdl	bdl	bdl	0.00	0.00	0.00	0.00	0.00	0.00	bdl	0.00	0.00
TOTAL	99.6	99.8	99.8	100.1	98.7	100.5	100.4	99.5	99.3	100.0	99.0	100.1
XMg(2)	91.8	91.6	91.6	91.2	90.9	90.8	91.7	92.5	92.0	93.7	96.0	94.4
Cr#(3)	34.5	20.7	35.1	30.0	31.7	36.5	29.0	28.2	27.4	29.3	24.8	25.7

(1): Hz = harzburgite

(2): XMg=100 Mg/(Fe^{2+}+Mg)

(3): Cr#=100 Cr/(Cr+Al)

bdl = below detection limit

TABLE 4: BULK ROCK COMPOSITONS FROM SAMPLES FROM BAY OF ISLAND OPHIOLITIC COMPLEX

		Blow-Me-Down									Table Mountain				North Arm								
Sample		BMD-11	BMD-12	BMD-13	BMD-15	BMD-17	BMD-18	BMD-19	BMD-22	BMD-23	TBL-01	TBL-03	TBL-04	TBL-05	8863	8928	89405	92111	92116	90365	8964	92160	92581
Rock [1]		Dun	Dun	Dun	Dun	Dun	Dun	Dun	Hz	Hz	Hz	Hz	Hz	Hz	Dun	Dun	Dun	Dun	Dun	Dun	Hz	Hz	Hz
SiO_2	%	34.2	34.7	34.4	34.2	34.4	34.2	35.1	38.4	38.9	38.8	39.8	39.7	39.7	35.6	35.6	34.4	36.1	34.6	35.8	38.5	39.5	40.2
TiO_2	%	0.03	0.03	0.02	0.02	0.02	0.03	0.03	0.02	0.02	0.02	0.02	0.02	0.02	0.03	0.03	0.02	0.05	0.02	0.02	0.02	0.02	0.02
Al_2O_3	%	1.91	0.7	0.64	0.57	1.48	2.40	0.66	0.49	0.38	0.51	0.78	0.5	0.94	1.32	1.32	0.56	0.6	1.17	0.34	0.62	0.94	0.38
Fe_2O_3	%	11.57	9.08	9.28	10.20	10.36	10.18	11.10	7.92	8.15	8.37	8.18	8.35	8.16	10.32	10.32	10.31	13.57	9.65	9.08	7.81	7.59	8.21
MnO	%	0.13	0.13	0.13	0.14	0.13	0.12	0.15	0.10	0.11	0.12	0.12	0.12	0.12	0.15	0.15	0.14	0.20	0.13	0.13	0.11	0.11	0.12
MgO	%	40.4	42.0	42.2	41.3	42.1	41.4	41.9	41.2	41.1	40.8	40.3	41.4	39.9	40.1	40.1	39.9	40.5	42.0	41.7	40.3	41.0	40.3
CaO	%	0.19	0.33	0.25	0.23	0.23	0.44	0.33	0.50	0.52	0.69	0.91	0.68	1.11	1.24	1.24	0.79	0.56	0.28	0.83	0.76	0.73	0.51
P_2O_5	%	0.006	0.006	0.005	0.005	0.006	0.008	0.008	0.006	0.005	0.004	0.004	0.002	0.004	0.007	0.007	0.006	0.007	0.005	0.004	0.005	0.004	0.004
LOI [2]	%	14.5	15.9	16.8	16.6	14.4	13.6	13.0	12.4	13.9	14.2	12.5	11.8	12.7	13.4	13.4	16.5	11.5	14.7	14.4	14.6	12.7	12.0
Sum	%	102.9	102.8	103.8	103.2	103.0	102.3	102.3	101.0	103.1	103.4	102.5	102.5	102.6	102.1	102.1	102.6	103.0	102.5	102.3	102.8	102.6	101.7
Ni	ppm	1834	2245	2020	1935	1833	2150	2152	2136	2237	2173	2115	2219	2129	1990	2510	2021	2025	2923	1897	2155	2122	2206
Cr	ppm	3219	4031	4164	2504	3669	3780	3450	3204	2665	2570	2516	2660	2519	3912	737	4271	2848	4908	5716	2441	2384	2975
Cu	ppm	2.0	15.3	0.3	0.5	19.3	19.9	28.7	5.0	16.0	7.3	11.5	5.8	19.2	13.0	2.1	152.1	39.3	169.9	1.2	2.6	2.4	2.8
S	ppm	66	35	79	41	337	116	482	239	139	252	158	67	172	231	33	894	287	799	133	77	24	44
Os	ppm	0.87	0.90	0.74	0.40	1.60	1.14	1.14	6.55	4.91	4.76	3.94	4.77	5.60	0.11	1.24	2.35	2.14	1.20	0.87	3.58	5.01	5.55
Ir	ppm	0.55	0.46	1.14	0.26	1.02	0.38	0.99	4.54	5.19	6.23	3.91	4.40	5.47	0.39	1.96	1.51	2.38	0.92	0.89	4.02	4.22	5.01
Ru	ppm	1.57	2.06	2.51	0.69	2.14	1.02	2.11	5.82	8.38	12.71	6.76	8.10	8.20	0.64	2.51	3.21	3.78	1.89	1.77	4.92	7.02	7.39
Rh	ppm	0.69	0.39	1.55	0.26	0.82	0.44	0.71	1.57	1.78	1.53	2.20	2.62	2.58	1.28	2.08	1.00	0.74	0.28	1.59	0.50	2.27	1.18
Pt	ppm	19.18	0.58	1.07	0.97	10.52	0.36	5.23	7.36	9.81	5.09	6.73	12.27	9.77	4.60	12.44	24.37	4.18	7.65	3.06	4.26	5.07	9.01
Pd	ppm	7.02	1.21	1.89	4.93	81.52	0.31	10.55	2.75	9.48	3.18	21.16	8.79	8.05	6.63	13.87	50.43	1.51	10.86	2.57	1.19	3.04	3.05
Bulk Mg # [3]		87	90	90	89	89	89	88	91	91	91	91	91	91	88	88	88	86	90	90	91	91	91

(1): Dun = dunite, Hz = harzburgite

(2): LOI = loss on ignition

(3): Bulk XMg = atomic 100 Mg/(Fe^{2+}+Mg)

TABLE 5: CALCULATED T AND fO_2

Sample	Location	Rock [1]	ΔfO_2(FMQ) [2]	T °C Ballhaus et al. (1991) [3]	T °C (B&K, 1990) [4]	T °C (B&K, 1990) [5]	T °C, Wells (1977) [6]
BMD-11	BMD	Dun	1.06	773	n.d.	n.d.	n.d.
BMD-12	BMD	Dun	0.09	756	n.d.	n.d.	n.d.
BMD-13	BMD	Dun	0.86	771	n.d.	n.d.	n.d.
BMD-15	BMD	Dun	1.15	812	n.d.	n.d.	n.d.
BMD-17	BMD	Dun	0.24	795	n.d.	n.d.	n.d.
BMD-18	BMD	Dun	0.96	891	n.d.	n.d.	n.d.
BMD-19	BMD	Dun	1.58	766	n.d.	n.d.	n.d.
8863	NAMM	Dun	1.13	907	n.d.	n.d.	n.d.
8928	NAMM	Dun	1.17	752	n.d.	n.d.	n.d.
89405	NAMM	Dun	0.60	710	n.d.	n.d.	n.d.
92111	NAMM	Dun	1.54	681	n.d.	n.d.	n.d.
92116	NAMM	Dun	0.36	731	n.d.	n.d.	n.d.
BMD-22	BMD	Hz	-0.59	739	909	n.d.	n.d.
BMD-23	BMD	Hz	-1.89	712	1093	n.d.	n.d.
TBL-01	TBL	Hz	-2.16	745	950	n.d.	n.d.
TBL-03	TBL	Hz	-2.22	745	1068	n.d.	n.d.
TBL-04	TBL	Hz	-2.01	734	933	n.d.	n.d.
TBL-05	TBL	Hz	-1.50	741	940	930	891
8964	NAMM	Hz	-2.49	727	1052	n.d.	n.d.
92160	NAMM	Hz	-1.45	734	912	1033	1051
92581	NAMM	Hz	-0.19	694	854	953	989

(1): Dun = dunites, Hz = harzburgite

(2): fO_2 estimates following the method of Ballhaus et al. (1991).

(3): Ballhaus et al. (1991) Ol-Spl Mg–Fe exchange thermometer.

(4): Brey and Köhler (1990) Ca-in-Opx thermometer

(5): Brey and Köhler (1990) two-pyroxene thermometer.

(6): Wells (1977) two-pyroxene thermometer.

n.d. - not determined, dunite samples do not contain pyroxenes to use a two pyroxene thermometry.

Chapter 2

Trace element study of olivine and spinel in cumulate dunite in the Bay of Island Ophiolitic Complex

ABSTRACT

We compared a measured trace element compositions for the bulk rock of dunite with a calculated trace element composition using the mineral chemistry and their abundance. This comparison allowed us to evaluate the trapped melt fraction and the melt composition in equilibrium with the dunite from the Bay of Island Ophiolitic Complex in Newfoundland. If the mineral chemistry reflects that of the time of their crystallization, the amount of trapped melt is calculated to be small, less than 1 % the samples.

The samples used in this study were collected from the thick dunitic sequence in the ultramafic cumulate layer from the Blow-Me-Down massif, one of massifs of the Bay of Ophiolitic Complex. The dunite samples contain olivine and Cr-spinel with minor sulphide and secondary magnetite. Serpentine replace olivine in the rims and along fractures. Bulk rock analysis of trace elements shows high concentrations of compatible and low concentration of incompatible elements.

INTRODUCTION

The parent melt composition of volcanic rocks can be evaluated from the bulk rock compositions. Alternatively, it is calculated from the composition of a phenocryst using the distribution coefficients of elements between the phase and melt. These methods are not directly applicable in the evaluation of parental melt for hollocrystalline rocks because the melt likely escaped from solidifying rocks. Some may have been incorporated as a trapped melt during their solidification. This trapped melt may form an overgrowth of major minerals or minute phases along grain boundaries of major phases. There is no direct way to ascertain the amount of trapped melt, yet, the amount of trapped melt fraction strongly influences the calculated concentrations of incompatible trace elements in the parental magmas because the

melt contains far higher concentrations of these elements than minerals. Therefore, it is important in evaluating the amounts of trapped melt because the concentrations of incompatible elements provide useful information related to the petrogenesis of magmas. This report evaluates the melt compositions and the trapped melt fraction of dunites based on trace element abundance, including rare earth elements, of constituent minerals and bulk rocks, and discusses different methods of calculating the hypothetical melt for plutonic rocks.

In this study, we selected dunite from the Bay of Island Ophiolitic Complex (BOIC). Dunite is a cumulate of mafic melt overlying harzburgitic rocks in the ophiolite complex and composed of olivine and Cr-spinel. Using the concentration data, we first compared the measured trace element chemistry in the bulk rock with a calculated trace element composition, using olivine and spinel data and their modal abundance. This comparison allowed us to calculate the trapped melt fraction and the melt composition in equilibrium with the dunite. The information is useful for the studies of other cumulate rocks.

SAMPLES

Two cumulate dunite samples (BMD-12 and BMD-17) were selected for this study after careful mapping and petrographic observations.

Sample BMD-12

The sample BMD-12 contains olivine (97.9 wt.%) and Cr-spinel (2.1 wt.%) and minor sulphide and magnetite. The modal abundance was calculated using Cr contents of bulk rock and Cr-spinel, assuming that all Cr is in Cr-spinel.

Olivine crystals are small (< 0.3 mm) and subhedral (Fig 1a). Olivine is replaced by serpentine in the rims and along fractures, and forming serpentine pseudomorphs. Abundant serpentine in the sample is supported by high value (15.9 wt.%) of loss on ignition (LOI; Table 1).

The Cr-spinel grains are usually small (< 0.2 mm) and opaque in thin sections under transmitted light. These small grains are round shaped and rimmed by secondary magnetite (Fig. 1b). Cr-spinel also forms coarse anhedral to subhedral grains. Minor amounts of Cr-spinel occur along grain boundaries and also as inclusion in olivine.

Disseminated fine-grained magnetite occurs together with serpentine as an alteration product of olivine. Discontinuous veinlets of magnetite form along grain boundaries of olivine and filling fractures in the rocks. High-temperature hydrous metasomatic minerals were not observed.

Sample BMD-17

Sample BMD-17 contains olivine (96.5 vol.%) and Cr-spinel (3.5 vol.%) and minor sulphide and magnetite. Olivine crystals are medium to small (< 0.5 mm) and subhedral to anhedral (Fig. 1c). As in sample BMD-12, olivine is commonly hydrated to serpentine. Serpentine partially to totally replaces olivine in the rims and along fractures of olivine, forming pseudomorphs. Fine-grained magnetite is disseminated within serpentine. The LOI (14.4 %) in this sample also supports the abundance of serpentine (Table 1).

Cr-spinel grains are more abundant and slightly larger (< 0.3 mm) than sample BMD-12. Cr-spinel are opaque in thin sections under transmitted light and forms coarse anhedral to subhedral grains (Fig. 1d), commonly replaced by magnetite along rims and fractures. Cr-spinel grains occur along grains boundaries and also as small inclusion in olivine. High-temperature hydrous metasomatic minerals were not observed.

ANALYTICAL METHODS

The concentration of major and minor elements in bulk rocks were determined at the University of Ottawa, using a Philips PW2400 sequential wavelength dispersive XRF. Major

elements were obtained from a fused bead made from a mixture of sample (1.5 g) with $LiBO_2$ (6.0 g) and $Li_2B_4O_7$ (1.5g) at ˜1050^oC.

Mineral compositions were determined using an automated 4 spectrometer CAMEBAX MBX electron probe (Carleton University) by the wavelength dispersive X-ray analysis method. Counting times were 15 seconds per element, except for Fe (20 s) and Ni (40 s). A 15 kV accelerating potential and a 20 nA beam current were applied. The calibration standards used were pure wollastonite (Si, Ca), synthetic spinel (Al), synthetic Cr_2O_3 (Cr), forsterite (Mg), synthetic $MnTiO_3$ (Mn, Ti), pure vanadium metal (V), albite (Na), fayalite (Fe in silicates) and synthetic Fe_3O_2 (Fe in oxides). Fe_2O_3 contents of spinel were determined assuming that stoichiometry is respected.

The trace element contents were determined by laser ablation ICP-MS at Memorial University of Newfoundland. The trace elements of minerals were determined in 50 μm thick sections, and those of the bulk rock were analyzed using fused beads prepared for the XRF. It consists of a Geolas 193 nm Excimer laser system linked to a Thermo-Finnigan Element II high-resolution ICP-MS. The laser beam sizes used in the LA-ICPMS were: 40 μm and 69 μm depending on the texture of the grains (Fig. 2). The concentrations of these elements were calculated from the count ratios of elements to Si in olivine grains and to Fe in Cr-spinel and bulk rocks, and the concentrations of SiO_2 and total Fe as FeO in the samples determined with an electron microprobe. References used are NIST 610, NIST 612, and BCR 2G. One cycle of analysis started with the measurement of background values by blocking the laser beam, followed by the laser abrasion of three references, followed by 12 samples. Each sample area was measured for at least three cycles while observing the ablation spectra. The trace elements analyzed for bulk rock were (Nb, La, Ce, Nd, Zr, Sm, Eu, Gd, Tb, Dy, Y, Er,

Yb, Lu, Ga, V and Sc); Cr-spinel (Nb, La, Ce, Nd, Zr, Sm, Eu, Gd, Tb, Dy, Y, Er, Yb, Lu, Ga, V, Sc and Co) olivine and serpentine (Nb, La, Ce, Nd, Zr, Sm, Eu, Ti, Gd, Tb, Dy, Y, Er, Yb, Lu, Zn, Ga, V, Sc, Co and Cr). Other elements (Mg, Al, S, Ca, Mn, Fe, Cu) were monitored during ablation to control the nature of the ablated material and the presence of included phases. The repeated analyses of references after every 12 areas suggest that the uncertainty is approximately 10%.

RESULTS

Bulk Rock

The dunite samples contain high concentrations of compatible elements, such as Ni (1830-2250 ppm), Cr (3670-4030 ppm). Bulk rock Mg# (atomic Mg/(Mg+total Fe) is high (0.89, 0.90). The samples contain low concentrations of moderately incompatible elements: CaO (0.23, 0.33 %), Al_2O_3 (0.7, 1.48 wt.%) and TiO_2 (0.018, 0.026 %). The concentrations of Sc, Ga and V in bulk rock are significant (Sc: 4.6-5.2 ppm; Ga: 1.2-1.8 ppm, V: 28-37 ppm). Y and Zr are low (Y: 0.02-0.102 ppm; Zr: 0.087-0.170 ppm). Rare earth elements (REE) are low in their concentrations, the total REE below 0.32 ppm.

Cr-Spinel

Different Cr-spinel grains in the individual samples have similar core compositions (Table 2). Chromium contents in the samples range from 32.7 % in sample BMD-12 to 17.1% in samples BMD-17; and TiO_2 from 0.09% to 0.41%. Cr-spinel in Sample BMD-12 has consequently higher value of Cr# (=Cr/[Cr+Al]) than BMD-17 (0.39 and 0.19 respectively). In both samples, the Fe^{3+} content is low ($YFe^{3+} = Fe^{3+}/[Al+Cr+Fe^{3+}]$, < 0.03). Values of XMg ($Mg/[Mg+Fe^{2+}]$) are similar in both samples (0.65 for BMD-12 and 0.71 for BMD-17) .

For trace elements (Table 5), Cr-spinel shows high values for V (922-938 ppm), Zn (1204-1573 ppm), Co (377-358ppm) and Ga (50-69 ppm). The contents of Sc range from 1.6 to 3.9 ppm. High-field strength elements, such as Zr and Nb, range from 1.5 to 17.6 ppm and 0.19 to 0.26 ppm respectively (Table 5). As in the bulk rock, REE show low concentrations below 0.24 ppm.

Olivine

Forsterite components of olivine (Fo=100 x Mg/[Mg+Fe]) in the dunite sample are 89 in sample BMD-17 and 90 in sample BMD-12 (Table 3). Other elements with significant concentrations include MnO (0.15-0.18 %), CaO (0.11-0.14 %) and NiO (0.29 to 0.32%). For trace elements (Table 6), Co show high concentrations ranging from 136 to 191 ppm. Cr (11-13 ppm) and Zn (28-36 ppm) also show significant concentrations. Vanadium in olivine is low (0.50-0.71 ppm). The concentrations of Sc range from 4.4 to 4.7 ppm, which are higher than the concentration in spinel. REE show low concentrations, below 0.22 ppm in total (Table 6).

Serpentine

Trace elements were also measured for serpentine (Table 7). The element Ga shows similar concentrations (0.17-0.28 ppm) as those observed in olivine. The elements Ti and Co are lower in concentrations than those in olivine (Ti > 0.004 ppm; Co: 68-113 ppm), whereas Sc, V and Cr concentration in serpentine are higher than olivine (Sc: 5.1-5.6 ppm; V: 0.9-1.1 ppm; Cr: 27-33 ppm), suggesting minor mobility of these elements during the hydration of dunite. Perhaps Cr was mobile during the oxidation of Cr-spinel to magnetite. The REE concentrations are below the detection limits.

DISCUSSION

Comparison of Trace Elements in Cr-Spinel, Olivine and Serpentine

Cr-spinel

Paktunc and Cabri (1995) determined the contents of Ga and Zn in Cr-spinel in mafic-ultramafic rocks from a variety of geological environments using a micro proton-induced X-ray excitation probe. The samples included Cr-spinel in ophiolitic complexes (including BOIC), layered intrusions, Alaskan-type complexes, komatiitic sills, Ni sulfide ores and metamorphosed mafic and ultramafic rocks. The concentrations of Ga and Zn in Cr-spinel in chromitites and dunites in BOIC range from 21-86 ppm, and 452-1640 ppm respectively, which are similar to our data, 50-69 ppm Ga and 1204-1570 ppm Zn.

Recently, Dare at al. (2009) determined the concentration of Ga in Cr-spinel from mafic-ultramafic rocks, including cumulate dunites in the South Sandwich islands and the Izu-Bonin arc, and the Semail ophiolite in Oman. The results show Ga concentrations ranging from 5.7 to 62.5 ppm. Comparing to our data, the Cr-spinel from BOIC dunite have concentrations similar to Cr-spinel in dunites from the Semail. Pagé and Barnes (2009) presented the concentrations of trace elements (Sc, V, Co, Zn, and Ga) in Cr-spinel from podiform chromitites of the Thetford Mines in Quebec, which is part of the Appalachian ophiolite south of the BOIC. They reported Sc ranging from 7.2 to 10.7 ppm, V from 417 to 525 ppm, Co from 166 to 386 ppm; Zn: 386-1286 ppm and Ga: 17.3-24.7 ppm. Compared to Cr-spinel in our dunite samples, the Cr-spinels in chromitite from Thetford Mines have lower concentrations of V and Ga, higher concentrations of Sc and similar concentrations of Co and Zn.

Olivine

De Hoog et al. (2009) showed that olivine in mantle peridotites in different locations (Fig. 3) have very similar concentrations of Co (87-143 ppm) and Zn (37.2-63 ppm), whereas Cr, V and Sc show wide variations; 1.45-604 ppm for Cr, 0.067-10.4 ppm for V and 0.38-1.89 ppm for Sc. Our samples show overall lower concentrations for Zn (28-36 ppm), Cr (11-13 ppm) and V (0.5-0.7 ppm); and higher concentrations of Sc (4.4-4.7 ppm) and Co (138-196 ppm) than those reported by De Hoog et al. (2009).

Serpentine

Deschamps et al. (2010 and 2012) reported trace element concentrations of serpentine in forearc serpentinites from the western Himalayas, and hydrated abyssal peridotites from Cuba and Dominican Republic. Serpentine contains high concentrations of fluid-mobile elements, such as U and Pb, but the concentrations of fluid-immobile elements are comparable to those of the precursor minerals of olivine and orthopyroxene. These immobile elements include Sc, Ti, Y and REE.

Bulk Rock Composition

The bulk rock composition was determined, but also calculated from the compositions of olivine and Cr-spinel. The concentration of an element (*e*) of a rock can be expressed as the sum of the modal abundance of minerals in fraction ϕ multiplied by the concentrations (C), of the element, of the mineral in the assemblage (Eq. 1).

$$C^{e}_{rock} = (\phi_{ol} * C^{e}_{ol}) + (\phi_{chr} * C^{e}_{chr}) \qquad (1)$$

Assuming that element (e) is present only in olivine and Cr-spinel in dunite, the concentration of the element in the rock is calculated from the modal abundances (ϕ) of olivine and Cr-spinel and the concentration of the element in these phases. Both measured

and calculated bulk rock compositions show concentrations of Sc, Ga and V slightly below the primitive mantle values (McDonough and Sun, 1995). The measured and calculated values also show low concentrations of immobile high-field strength elements, such as Ti, Zr and Nb, and REE (Fig. 4; Table 8).

Although measured and calculated bulk rock compositions show a similar primitive-mantle normalized profile (Fig. 4), there are differences. The measured bulk compositions have overall higher concentration of incompatible elements than the calculated compositions (Fig. 4). For example, measured concentrations of Ti are significantly higher than the calculated, for both samples (108 and 156 ppm instead of calculated 24 and 72 ppm). There are several possible explanations. One possible explanation is an introduction of elements during serpentinization. This may be explained by Ti in magnetite, which commonly has high concentration of Ti. Serpentinization of olivine produces serpentine and magnetite and Ti was possibly incorporated into magnetite from the external source during the hydration process.

Another possible explanation for high measured concentrations of incompatible elements is the existence of trapped melt fraction (TMF) in the rock. The trapped melt then crystallizes to produce overgrowths on cumulus crystals, plus additional interstitial phases enriched in components excluded from the cumulus phases. This trapped melt, may form minute phases along grain boundaries of major phases. To evaluate this possibility, the composition of the hypothetical melt is calculated.

For Zn, Co and Cr, the calculated concentrations are slightly higher than the measured concentrations, but the difference is less than 17 ppm for Zn, 70 ppm for Co and 506 ppm for Cr which is within the analytical uncertainty of these elements.

Hypothetical Melt Composition

The composition of melt in equilibrium with olivine and Cr-spinel is calculated from the compositions of minerals, modal abundances of minerals, mineral/melt partition coefficients (Eq. 2). In this equation we assumed no TMF.

$$C^{e}_{melt} = (\phi_{ol} * D^{e}_{ol}) + (\phi_{chr} * D^{e}_{chr}) \qquad (2)$$

$$D_{ol} = C_{sol}/C_{melt}$$

$$D_{chr} = C^{chr}_{sol}/C^{chr}_{melt} \qquad (3)$$

By substituting equations of this Eq. 3 into Eq. 2 we can eliminate all but one of the unknowns (C^{e}_{melt}). The final equation (Eq. 4) allows us to calculate the hypothetical melt composition that was in equilibrium with the dunite samples.

$$C^{e}_{melt} = \phi_{ol} * (C^{e}_{sol}/D^{e}_{ol}) + \phi_{chr} * (C^{e}_{sol}/D^{e}_{chr}) \qquad (4)$$

The hypothetical melt compositions are also calculated following the method by Bédard (1994) which requires the bulk rock compositions, modal abundance of minerals and distribution coefficients of elements between minerals and melt.

Distribution Coefficients (*D*)

Distribution coefficients (*D*) between crystal to melt have been evaluated through experiments and empirical observation. Bédard (1994) compiled several *D* values for olivine and spinel. The lack of a more recent data for *D* values for olivine and spinel makes the study from Bédard 1994 still a reliable source for *D* values. Bédard (2005) compiled again *D* values for olivine. Since this is one the most recent and consistent work to review the values between olivine and silicate melt, this study uses the *D* values for olivine from Bédard (2005). Most recently Pagé and Barnes (2009) evaluated *D* values for trace elements from ultramafic rocks from Thetford Mine Ophiolite in Quebec. The study also compiled previously available *D*

values for Cr-spinel. We also used *D* values obtained from Pagé and Barnes (2009). Table 9 shows the distribution coefficients used in our study.

Vanadium has a variety of valences from +2 to +5 in natural environments and its distribution coefficient is strongly influenced by the valence. Divalent and trivalent V are compatible with silicate and oxide minerals, but pentavalent V^{5+} is not (e.g., Mallmann and O'Neil, 2009). Therefore, the distribution coefficient of the bulk V varies depending on oxidation conditions by several orders of magnitude. Considering our samples crystallized under oxidizing conditions close to the quartz+faylite+magnetite buffer, (QFM -0.1 and +0.05 respectively for BMD-12 and BMD-17), we chose 0.0075 for the *D* value of olivine and 7.73 for that of Cr-spinel based on the relationship between *D* and fO_2 by Mallmann and O'Neil (2009). The choice of the *D* value for olivine does not make any significant difference at fO_2 around FMQ buffer because the values are 0.0068 at QFM-0.5 and 0.0085 at QFM+0.5, but the value is sensitive for Cr-spinel. It will be 5.6 at QFM-0.5 and 7.8 at QFM+0.5.

Calculated Composition of the Hypothetical Melt.

We calculated the composition of the hypothetic melt in equilibrium with the dunite based on the abundance of minerals, their mineral chemistry, and their *D* values between melt and mineral using the equations 2 to 4 and the results are listed in Table 10 and plotted in Figure 5. All elements show similar concentrations for the two samples: V (68-96 ppm), Ga (0.88-2.56 ppm), Co (36-49 ppm), Zn (17-18 ppm), Zr (5.5-9.5 ppm) and Nb (1.5-1.7 ppm). The hypothetic melt is rich in Sc (27-30 ppm) and Y (7.8-19.6 ppm) compared to primitive mantle values and low Cr (39-45 ppm) and Ti (163-611 ppm). The REE also show high concentration in the calculated melt than the primitive mantle values, with Sm and Eu ranging from 30-87 ppm and 18-51 ppm respectively.

The hypothetical melt shows a distinct subduction-related geochemical signature where the concentrations of high-field strength elements are low. The lack of Eu anomalies suggests the absence of plagioclase at the source mantle and no prior crystallization of plagioclase. This is supported by the lack of plagioclase in harzburgitic rocks in the BOIC. Harzburgite rocks are present underlying dunite bodies in the BOIC and considered to be the source for the parental melt of dunite.

It has been suggested that the parental melt for dunites is boninitic by Varfalvy et al., (1997) and Bédard (2007). But, the composition of the hypothetical melt for the dunite samples is quite different from the average of boninites from the Bonin-Mariana forearc (Pearce et al., 1992).

The Hypothetical Melt Composition Calculated by the Method Proposed by Bédard (1994).

The composition of the hypothetic melt for the two dunite samples (BMD-12, BMD 17) was also calculated following the procedure described by Bédard (1994). The procedure uses the bulk rock compositions, the abundance of minerals, their *D* values and a trapped melt fraction (TMF). The abundance of minerals and their *D* values are identical to those used in the first method. Bédard (1994) suggested that TMF values may vary from 0 to 5 % in most rocks. We used 0 % as the value of TMF for the calculation. The rational for this assignment is described in the section of TMF.

The first and second methods yielded significantly different compositions of the hypothetical melt (Fig. 6, Table 11). The Bédard's method assuming 0 % TMF yielded lower concentrations of REE, and higher concentrations for V, Co, Cr and Ti than the first method using mineral chemistry data. Both methods gave similar concentrations for Ga and Zr (Fig. 6). Since the two methods used identical D values, uncertainty of D values cannot explain

the difference. The difference in the results between these two methods of calculation can be explained by presence of serpentine in the bulk rocks or by the incorporation of the trapped melt into olivine during solidification.

Bulk rock contains serpentine, therefore the melt composition obtained from the bulk rock is being influenced by the trace element concentrations of serpentine in the rock. But the concentration of trace element in serpentine measured in this study do not support this possibility due to the low concentrations of V, Co, Cr and Ti in serpentine (Table 7).

The second possibility, olivine composition may have changed during solidification by incorporation of the trapped melt, therefore not reflecting the composition of melt. However, the compositions of olivine is similar to that of the mantle (Fig. 3).

Trapped Melt Fraction

The trapped melt fraction is calculated for the dunite samples by comparing the measured compositions in the bulk rock and calculated from the compositions of olivine, Cr-spinel and the hypothetical melt. The trapped melt fraction of an element (*e*) in a rock can obtained using equation (5):

$$C_{rock} = [(\phi_{ol} * C_{ol}) + (\phi_{chr} * C_{chr})] + TMF * C_{melt} \quad (5)$$

This is rearranged to obtain the TMF for each element (e).

$$TMF = \{C_{rock} - [(\phi_{ol} * C_{ol}) + (\phi_{chr} * C_{chr})]\} / C_{melt} \quad (6)$$

The results show that dunite rocks from BOIC have very small fractions of trapped melt (Table 12). The values obtained from REE are all small. The use of other elements, such as V, yielded equally small TMF values, lower than 1 % (Table 12). Some trace elements yielded small, but negative values for the TMF. It is not surprising considering

uncertainties of 10 % for the concentration of the element in the rock and also the distribution coefficients.

SUMMARY

Both measured and calculated trace elements composition of the bulk rocks are similar, with high concentrations of compatible and low concentration of incompatible elements. The similar results observed allow to conclude that the trapped melt fraction in the rock was very small and negligible or the trapped melt fraction was incorporated into olivine.

Overall the measured trace element concentrations are higher than the calculated ones; the exceptions are elements such as Cr, Co and Zn, elements that were incorporated into serpentine during the hydration of olivine.

Cr-spinel from BOIC dunite has the major, minor and trace element composition similar to that in dunites from the Semail ophiolite in Oman. Cr-spinels in chromitite from Thetford Mines have lower concentrations of V and Ga, higher concentrations of Sc and similar concentrations of Co and Zn.

The hypothetical melt in equilibrium with dunites from BOIC has high concentration of incompatible elements, which is unrealistic high. The D values used in this study may not be accurate enough and may be the reason for these high concentrations. Another possibility, the composition of olivine changed to incorporate trace elements in trapped melt. Therefore, the melt composition calculated from the bulk rock give a more realistic melt composition. But the bulk rock composition can be also modified because of serpentinization of the minerals.

Ultramafic rocks contain very low concentrations of incompatible elements. Therefore, their concentrations are susceptible to modification during alteration. Furthermore, olivine is commonly hydrated to incorporate fluid-mobile elements. Estimates

of a hypothetical melt based on the bulk rock compositions may lead to erroneous results. More work has to be conducted in order to better understand the difference of concentration obtained between these two methods.

Our work was the first study documenting the trace elements in dunite and clearly suggest a further work on D values is required.

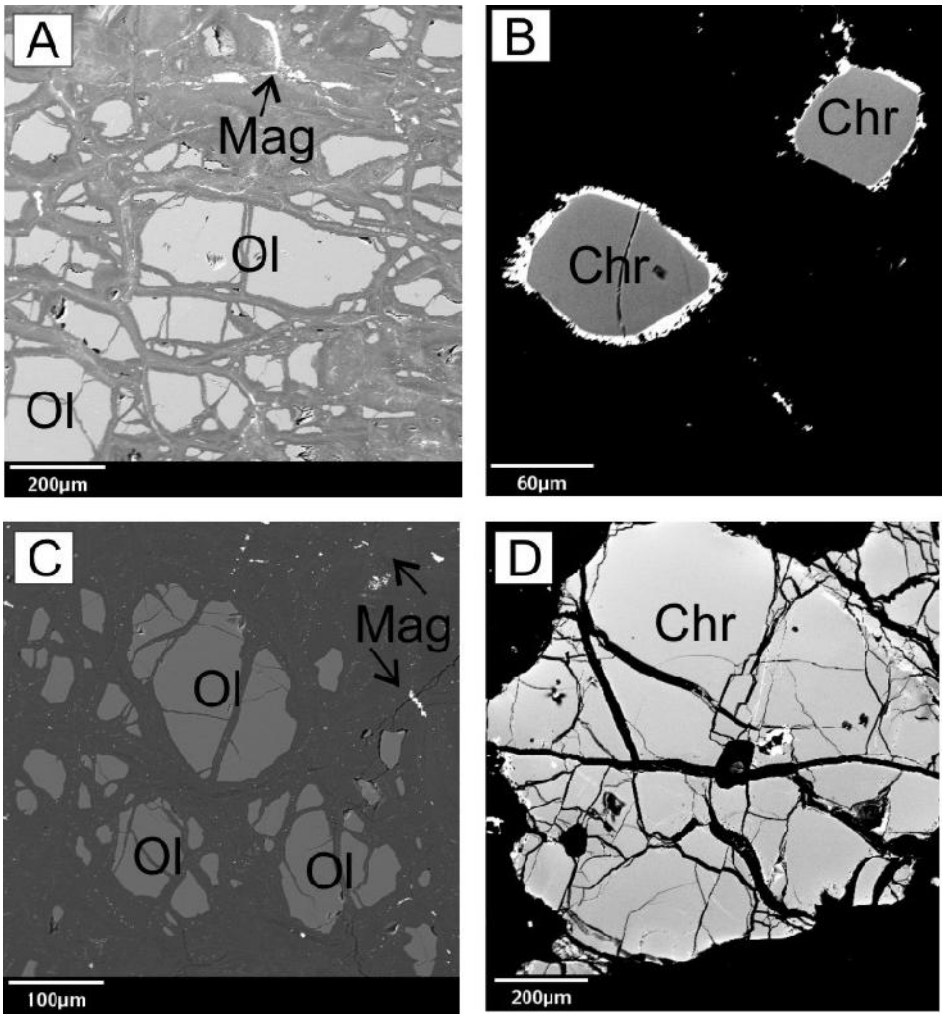

Figure 1: Back-scattered electron images of BOIC dunites. (A) Sample BMD-12 showing olivine grains (Ol) and fine grained magnetite (Mag). (B) Cr-spinel (Chr) rimmed by magnetite (Mag) in Sample BMD-12. (C) Sample BMD-17 with olivine (Ol) grains and fine grained magnetite (Mag). (D) A subhedral Cr-spinel grain in sample BMD-17.

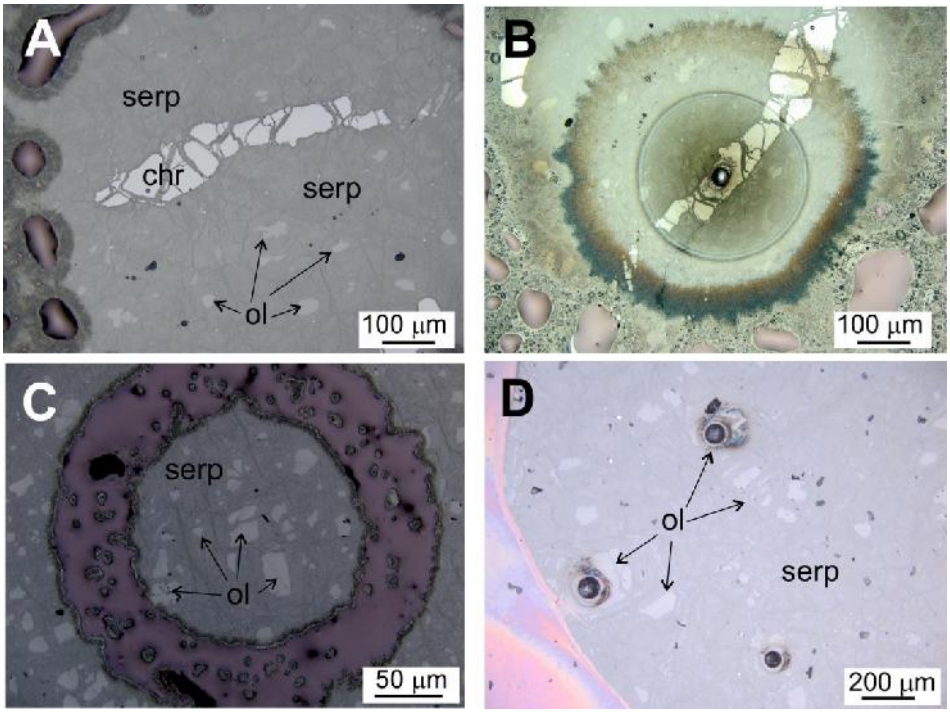

Figure 2: Incident light photomicrograph showing Cr-spinel grains (chr) (A) before carbon coating (B) after the analysis with LA-ICPMS of spinel grain in sample BMD-12. The size of laser beam was 52 μm, (C) before carbon coating and (D) after the analysis with LA-ICPMS of spinel grains in sample BMD-17. The size of laser beam was 69 μm. Olivine (ol) in lighter gray in the matrix of serpentine (serp).

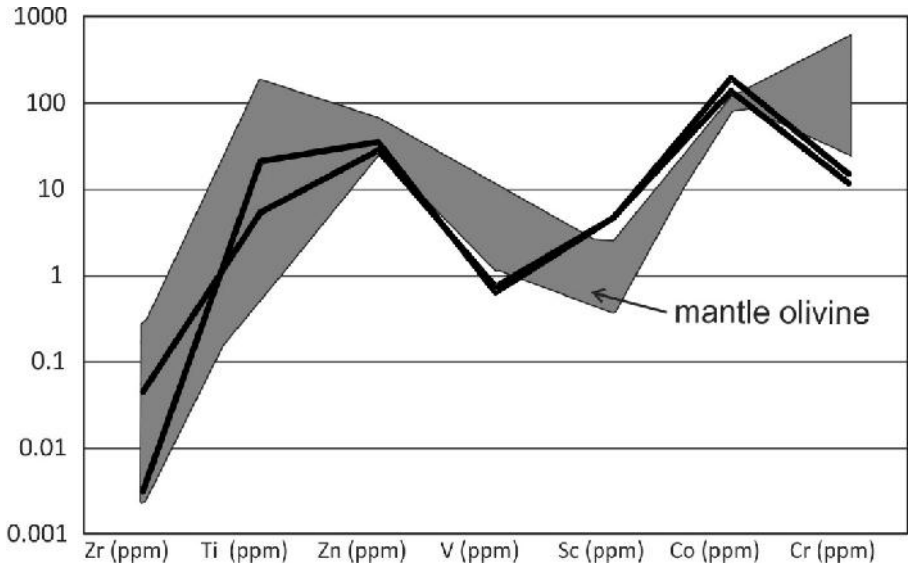

Figure 3: Trace element concentration (black solid lines) of dunite samples BMD-12 and BMD-17. Data for mantle olivines are from De Hoog et al. (2009).

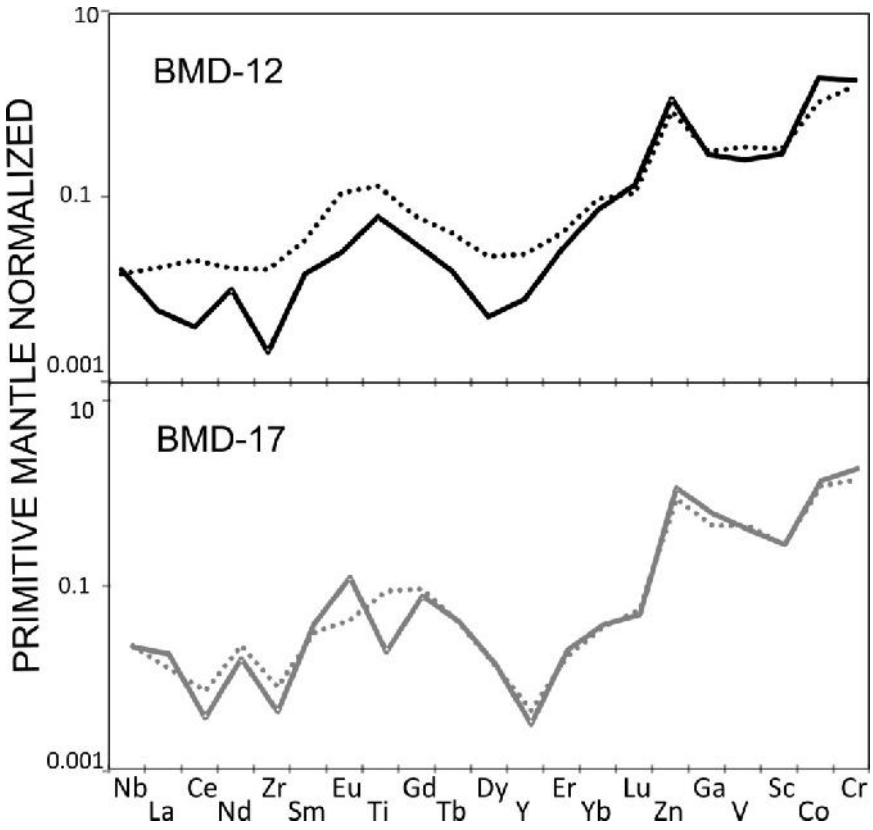

Figure 4: Calculated trace element composition (solid lines) dunite based on the composition of olivine and Cr-spinel and their modal abundance. The trace element pattern is compared to the measured trace element (dashed lines) composition of dunite samples BMD-12 and BMD-17. Primitive mantle values are from McDonough and Sun (1995).

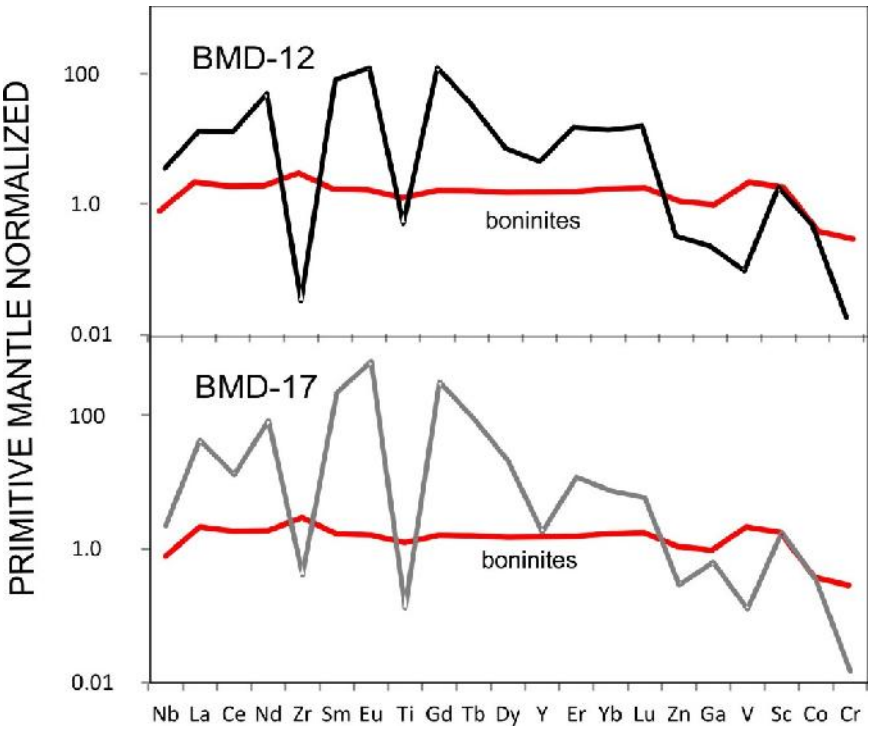

Figure 5: Trace element abundance of the hypothetical melt for dunite samples BMD-12 and BMD-17 calculated from the distribution coefficients of elements between minerals and melt, the compositions of olivine and Cr-spinel, and their abundance. The trapped melt fraction is assumed to be zero in the calculation. The primitive mantle values are from McDonough and Sun (1995). Average of boninite concentrations from the Izu-Bonin forearc from Pearce et al. (1992).

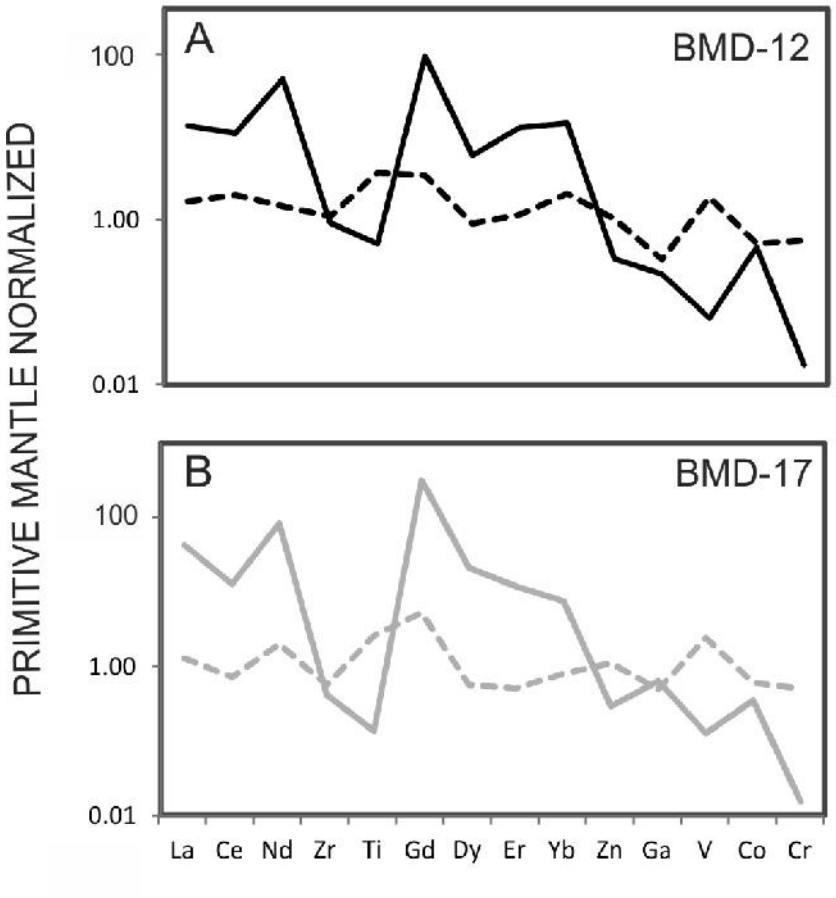

Figure 6: (A & B): The compositions of the hypothetical melt for dunite samples calculated by two different methods. One method (solid line) uses the mineral chemistry of olivine and Cr-spinel, their abundance and *D* values between minerals and melt. The second method (dashed line) is based on the procedure described by Bédard (1994), which uses the bulk rock composition, the abundance of minerals, and their *D* values. The same mineral abundance and *D* values are used for the two methods.

TABLE 1: BULK ROCK COMPOSITONS OF THE DUNITE SAMPLES

Sample	SiO_2	TiO_2	Al_2O_3	$FeO^{(1)}$	MnO	MgO	CaO	K_2O	P_2O_5	$LOI^{(2)}$	Sum	Bulk Mg # $^{(3)}$	Zn	Co
	%	%	%	%	%	%	%	%	%	%	%		ppm	ppm
BMD-12	34.7	0.026	0.7	9.1	0.126	42.0	0.33	0.007	0.006	15.91	102.8	90.2	49	123
BMD-17	34.4	0.018	1.48	10.4	0.128	42.1	0.23	0.004	0.006	14.35	103.1	88.9	53	144

(1): Fe total as Fe_O (3): Bulk Mg# = atomic Mg*100/(Mg + Fe_2O_3).

(2): LOI = loss on ignition

TABLE 2: COMPOSITONS OF REPRESENTATIVES SPINEL GRAINS OF THE DUNITE SAMPLES

Sample	SiO_2	TiO_2	Al_2O_3	Cr_2O_3	$FeO^{(1)}$	MnO	MgO	CaO	TOTAL	$YFe^{3}+^{(2)}$	$XMg^{(3)}$	$Cr\#^{(4)}$
	%	%	%	%	%	%	%	%	%			
BMD-12	0.03	0.41	33.6	32.69	16.81	0.24	15.04	<0.01	98.8	0.032	0.65	0.39
BMD-17	0.05	0.09	48.4	17.10	15.35	0.12	17.49	0.02	98.6	0.032	0.71	0.19

(1): Fe total as FeO (3): Mg#=100 Mg/(Fe^{2+}Mg)

(2): YFe^{3+} =$Fe3^{+}$/(Al+Cr+$Fe^{3.}$ (4): Cr#=100 Cr/(Cr+Al)

TABLE 3: COMPOSITONS OF REPRESENTATIVES OLIVINE OF THE DUNITE SAMPLES

Sample	SiO_2	Al_2O_3	FeO[1]	MnO	MgO	NiO	CaO	TOTAL	Fo[2]
BMD-12	40.6	0.01	9.1	0.18	48.9	0.32	0.11	99.3	90
BMD-17	40.5	<0.01	10.8	0.15	48.3	0.29	0.14	100.2	89

(1): Fe total as FeO

(2): Fo= forsterite component = 100 Mg/(Mg+Fe).

TABLE 4: MEASURED TRACE ELEMENTS IN BULK ROCK

Sample	Nb (ppm)	La (ppm)	Ce (ppm)	Nd (ppm)	Zr (ppm)	Sm (ppm)	Eu (ppm)	Gd (ppm)	Tb (ppm)	Dy (ppm)	Y (ppm)	Er (ppm)	Yb (ppm)	Lu (ppm)	Ga (ppm)	V (ppm)	Sc (ppm)
BMD 12	0.010	0.011	0.034	0.021	0.170	0.014	0.017	0.034	0.004	0.015	0.102	0.018	0.042	0.007	1.2	28	5.2
BMD 17	0.008	0.008	0.019	0.029	0.087	0.013	0.007	0.052	0.004	0.010	0.020	0.008	0.016	0.004	1.8	37	4.6

TABLE 5: TRACE ELEMENTS IN CR-SPINEL

Sample	Nb (ppm)	La (ppm)	Ce (ppm)	Nd (ppm)	Zr (ppm)	Sm (ppm)	Eu (ppm)	Gd (ppm)	Tb (ppm)	Dy (ppm)	Y (ppm)	Er (ppm)	Yb (ppm)	Lu (ppm)	Zn (ppm)	Ga (ppm)	V (ppm)	Sc (ppm)	Co (ppm)
BMD-12	0.26	0.01	0.028	0.0877	17.6	0.0055	0.007	0.0236	0.0064	0.012	0.021	0.037	0.006	0.0005	1573	50	922	3.9	358
BMD-17	0.19	0.004	0.025	0.0289	1.5	0.0098	0.0043	0.0313	0.0031	0.004	0.025	0.014	0.007	0.0018	1204	69	938	1.6	377

TABLE 6: TRACE ELEMENTS IN OLIVINE

Sample	Nb (ppm)	La (ppm)	Ce (ppm)	Nd (ppm)	Zr (ppm)	Sm (ppm)	Eu (ppm)	Ti (ppm)	Gd (ppm)	Tb (ppm)	Dy (ppm)	Y (ppm)	Er (ppm)	Yb (ppm)	Lu (ppm)	Zn (ppm)	Ga (ppm)	V (ppm)	Sc (ppm)	Co (ppm)	Cr (ppm)
BMD-12	0.012	0.0039	0.0054	0.012	0.003	0.006	0.004	21	0.013	0.002	0.003	0.040	0.010	0.035	0.008	36	0.03	0.50	4.7	191	13
BMD-17	0.009	0.009	0.007	0.022	0.044	0.016	0.011	5	0.041	0.004	0.010	0.016	0.009	0.018	0.004	28	0.13	0.71	4.4	136	11

TABLE 7: TRACE ELEMENTS IN SERPENTINE

Sample	Nb (ppm)	La (ppm)	Ce (ppm)	Nd (ppm)	Zr (ppm)	Sm (ppm)	Eu (ppm)	Ti (ppm)	Gd (ppm)	Tb (ppm)	Dy (ppm)	Y (ppm)	Er (ppm)	Yb (ppm)	Lu (ppm)	Zn (ppm)	Ga (ppm)	V (ppm)	Sc (ppm)	Co (ppm)	Cr (ppm)
BMD-12	0.004	<0.007	<0.005	<0.025	<0.125	<0.007	<0.008	0.004	<0.020	<0.007	<0.015	0.0437	<0.004	0.04471	<0.005	31	0.28	0.94	5.1	68	33
BMD-17	<0.009	<0.003	<0.005	<0.025	<0.125	<0.007	<0.008	0.001	<0.020	<0.007	<0.013	0.0162	<0.004	0.01192	<0.005	30	0.17	1.11	5.6	113	27

TABLE 8: COMPARISON BETWEEN MEASURED AND CALCULATED COMPOSITION OF DUNITE

BMD-12	Nb (ppm)	La (ppm)	Ce (ppm)	Nd (ppm)	Zr (ppm)	Sm (ppm)	Eu (ppm)	Ti (ppm)	Gd (ppm)	Tb (ppm)	Dy (ppm)	Y (ppm)	Er (ppm)	Yb (ppm)	Lu (ppm)	Zn (ppm)	Ga (ppm)	V (ppm)	Sc (ppm)	Co (ppm)	Cr (ppm)
MET[1]	0.0095	0.011	0.034	0.021	0.170	0.014	0.017	156	0.034	0.004	0.015	0.102	0.018	0.042	0.007	49	1.21	28	5.2	123	4114
CTE[2]	0.0171	0.004	0.006	0.014	0.373	0.006	0.004	72	0.013	0.002	0.003	0.039	0.010	0.034	0.008	68	1.08	20	4.7	194	4710
Difference	**-0.0076**	**0.007**	**0.029**	**0.007**	**-0.202**	**0.008**	**0.013**	**83.7**	**0.020**	**0.002**	**0.012**	**0.063**	**0.007**	**0.008**	**-0.001**	**-19**	**0.132**	**8.2**	**0.5**	**-71**	**-596**
BMD-17	Nb (ppm)	La (ppm)	Ce (ppm)	Nd (ppm)	Zr (ppm)	Sm (ppm)	Eu (ppm)	Ti (ppm)	Gd (ppm)	Tb (ppm)	Dy (ppm)	Y (ppm)	Er (ppm)	Yb (ppm)	Lu (ppm)	Zn (ppm)	Ga (ppm)	V (ppm)	Sc (ppm)	Co (ppm)	Cr (ppm)
MTE[1]	0.0151	0.008	0.013	0.029	0.087	0.013	0.007	108	0.052	0.004	0.010	0.020	0.008	0.016	0.004	53	1.82	37	4.6	144	3719
CTE[2]	0.0149	0.009	0.007	0.022	0.096	0.016	0.010	24	0.040	0.004	0.010	0.016	0.009	0.017	0.004	69	2.49	33	4.3	144	4135
Difference	**0.0003**	**-0.001**	**0.005**	**0.007**	**-0.009**	**-0.003**	**-0.004**	**84.13**	**0.011**	**0.000**	**-0.001**	**0.003**	**-0.002**	**-0.001**	**0.000**	**-16**	**-0.666**	**3.5**	**0.262**	**0**	**-417**

(1): Measured composition in the bulk rock

(2): Calculated composition using averages values from tables 5 and 6.

TABLE 9: *D* VALUES USED IN THE STUDY

Element	*D* olivine	*D* spinel	Element	*D* olivine	*D* spinel
Nb	0.01[(1)]	0.01[(1)]	**Y**	0.002(1)	0.01(1)
La	0.00044[(1)]	0.0006(1)	**Er**	0.00174(1)	0.003(1)
Ce	0.0003[(1)]	0.0006(1)	**Yb**	0.00522(1)	0.0045(1)
Nd	0.0002[(1)]	0.0006(1)	**Lu**	0.00852(1)	0.0045(1)
Zr	0.01026[(2)]	0.04(1)	**Zn**	2.564(2)	6.9(3)
Sm	0.00018[(1)]	0.0006(1)	**Ga**	0.09745(2)	1.83(3)
Eu	0.0002[(1)]	0.0006(1)	**V**	0.097(4)	7.73(4)
Ti	0.038[(2)]	0.753(3)	**Sc**	0.158(2)	0.198(3)
Gd	0.00025(1)	0.0006(1)	**Co**	4(1)	3.83(1)
Tb	0.000475(1)	0.00105(1)	**Cr**	0.6(1)	200(1)
Dy	0.0007(1)	0.0015(1)			

(1): from Bédard, 1994

(2): from Bédard, 2005

(3): from Pagé and Barnes, 2009

(4): from Mallmann and O'Neil, 2009

TABLE 10: MELT COMPOSITION

Element	Nb (ppm)	La (ppm)	Ce (ppm)	Nd (ppm)	Zr (ppm)	Sm (ppm)	Eu (ppm)	Ti (ppm)	Gd (ppm)	Tb (ppm)	Dy (ppm)	Y (ppm)	Er (ppm)	Yb (ppm)	Lu (ppm)	Zn (ppm)	Ga (ppm)	V (ppm)	Sc (ppm)	Co (ppm)	Cr (ppm)
BMD-12	1.7	8.9	19	64	9.5	30	18	611	52	3.4	4.1	19.6	5.8	6.5	0.95	18	0.88	68	30	49	45
BMD-17	1.5	21.0	23	107	5.5	87	51	163	158	8.91	14.3	7.8	5.3	3.3	0.41	17	2.56	96	27	36	39

TABLE 11: MELT COMPOSITION USING BÉDARD (1994) METHOD.

Sample ID	Rock type	La (ppm)	Ce (ppm)	Nd (ppm)	Zr (ppm)	Ti (ppm)	Gd (ppm)	Dy (ppm)	Er (ppm)	Yb (ppm)	Zn (ppm)	Ga (ppm)	V (ppm)	Co (ppm)	Cr (ppm)
BMD-12	Dun	1.08	3.3	1.8	11	4482	1.87	0.60	0.50	0.91	56	1.3	151	54	1451
BMD-17	Dun	0.83	1.2	2.5	6	3103	2.86	0.38	0.22	0.35	61	2.0	197	63	1311
8863	Dun	18.58	39.3	15.7	2966	5167	3.33	2.38	1.57	1.95	57	1.6	242	48	353

TABLE 12: TRAPPED MELT FRACTION

Element	Nb (ppm)	La (ppm)	Ce (ppm)	Nd (ppm)	Zr (ppm)	Sm (ppm)	Eu (ppm)	Ti (ppm)	Gd (ppm)	Tb (ppm)	Dy (ppm)	Y (ppm)	Er (ppm)	Yb (ppm)	Lu (ppm)	Zn (ppm)	Ga (ppm)	V (ppm)	Sc (ppm)	Co (ppm)	Cr (ppm)
BMD-12	-4.5E-03	7.9E-04	1.5E-03	1.1E-04	-0.021	2.7E-04	7.1E-04	0.137	3.9E-04	6.7E-04	3.0E-03	3.2E-03	1.3E-03	1.2E-03	-0.001	-1.03	0.15	0.12	0.017	-1.47	-13.13
BMD-17	2.0E-04	-4.0E-05	2.3E-04	6.3E-05	-0.002	-3.4E-05	-7.2E-05	0.517	7.2E-05	-3.0E-05	-3.7E-05	4.5E-04	-3.2E-04	-3.5E-04	0.001	-0.96	-0.26	0.04	0.010	0.001	-10.74

SUMMARY OF CONCLUSIONS

Chapter 01

- Bulk rock chemistry, mineral chemical data and calculated fO_2 show that BOIC harzburgites are refractory mantle residues after partial melting, whereas the PGE abundance suggests a cumulate origin for BOIC dunites.
- The BOIC is interpreted as the vestiges of an ephemeral, peri-continental oceanic lithosphere which formed at a slow spreading ridge, presumably in the vicinity of an arc.
- Moderate Cr# values of spinel and the overall geochemically signature of BOIC harzburgites record melt extraction beneath the spreading ridge, whereas high Cr# values in Cr-spinel likely formed after the initiation of subduction.
- The compositional variation of Cr-spinel reflects a change in the tectonic settings during BOIC formation and a progressive depletion in the mantle through melt extraction in a subduction setting.

Chapter 02

- Both measured and calculated trace elements composition of the bulk rocks are similar. Overall the measured trace element concentrations are higher than the calculated ones. The amount of trapped melt in the rocks is calculated to be very small, less than 1 % for all elements in both dunite samples.
- Cr-spinel from BOIC dunite has the major, minor and trace element composition similar to that in dunites from the Semail ophiolite in Oman. Cr-spinels in chromitite from Thetford Mines have lower concentrations of V and Ga, higher concentrations of Sc and similar concentrations of Co and Zn.

REFERENCES

Anonymous, 1972, Penrose Field Conference on ophiolites: Geotimes, v. 17, p. 24–25.

Arai, S., 1994, Characterization of spinel peridotites by olivine-spinel compositional relationships: review and interpretation. Chemical Geology, v. 111, p. 191–204.

Arai, S., Ishimaru, S., Okrugin, V.M., 2003, Metasomatized harzburgite xenoliths from Avacha volcano as fragments of mantle wedge of the Kamchatka arc: implication for the metasomatic agent. Island Arc, v. 12, p. 233–246.

Ballhaus, C., Berry, R.F., Green, D.H., 1991, High pressure experimental calibration of the olivine-orthopyroxene-spinel oxygen geobarometer: implications for the oxidation state of the upper mantle. Contributions to Mineralogy and Petrology, v. 107, p. 27–40.

Barnes S. J., Lesher C. M., Keays R. R., 1995, Geochemistry of mineralised and barren komatiites from the Perseverance nickel deposit, Western Australia. Lithos, v. 34, p. 209–234.

Barnes S. J., and Picard C. P., 1993, The behavior of platinum-group elements during partial melting, crystal fractionation, and sulphide segregation: An example from the Cape Smith Fold Belt, northern Quebec. Geochimica et Cosmochimica Acta, v. 57, p. 79–87.

Batanova, VG, G Suhr, A V Sobolev, 1998, Origin of geochemical heterogeneity in the mantle peridotites from the Bay of Islands ophiolite, Newfoundland, Canada: Ion probe study of clinopyroxenes: Geochimica et Cosmochimica Acta, v. 62, p. 853-866.

Bédard, J.H, 1991, Cumulate recycling and crustal evolution in the Bay of island Ophiolite. Journal of Geology, v. 99, p. 225-249.

Bédard, J.H., 1993, Oceanic crust as a reactive filter: synkinematic intrusion, hybridization, and assimilation in an ophiolitic magma chamber, western Newfoundland: Geology, v. 21, p. 77-80.

Bédard, J.H., 1994, A procedure for calculating the equilibrium distribution of trace elements among the minerals of cumulate rocks, and the concentration of trace elements in the coexisting liquids: Chemical Geology, v. 118, p. 143-153.

Bédard, J., H., 2005, Partitioning coefficients between olivine and silicate melts. Lithos, v. 83, p. 394-419.

Bédard, J.H., 2007, Trace element partitioning coefficients between silicate melts and orthopyroxene: Parameterizations of D variations. Chemical Geology, v. 244[1-2], p. 263-303.

Bédard, J.H., and Hébert, R., 1996, The lower crust of the Bay of Islands ophiolite, Canada: Petrology, mineralogy, and the importance of syntexis in magmatic differentiation. Journal of Geophysical Research, v. 101, p. 25105-25124.

Bédard, J.H., and Hébert, R., 1998, Formation of chromitite by assimilation of crustal pyroxenites and gabbros into peridotitic intrusions: North Arm Mountain massif, Bay of Islands ophiolite. Journal of Geophysical Research, v. 103, p. 5165-5184.

Bédard, J.H., and Escayola, M.., 2010, The Advocate ophiolite mantle, Baie Verte, Newfoundland: regional correlations and evidences for metasomatism. Canadian Journal of Earth Sciences, v. 47, p. 237-253.

Brenan, J.M., 2003, Effects of fO_2, fS_2, temperature, and melt composition on Fe-Ni exchange between olivine and sulphide liquid: Implications for natural olivine–sulphide assemblages. Geochimica et Cosmochimica Acta, V. 67, n. 14, p. 2663–2681.

Brenan, J. M., McDonough, W. F., Ash R., 2005, An experimental study of the solubility and partitioning of iridium, osmium and gold between olivine and silicate melt. Earth and Planetary Science Letters, v. 237, p. 855–72.

Brey, G.P., and Köhler, T., 1990, Geothermobarometry in four-phase lherzolites: II. New thermobarometers, and practical assessment of existing thermobarometers. Journal of Petrology, v. 31, p. 1353–1378.

Bryndzia, L.T., and Wood, B.J., 1990, Oxygen thermobarometry of abyssal spinel peridotites: the redox state and C–H–O volatile composition of the Earth's sub-oceanic upper mantle. The American Journal of Science, v. 290, p. 1093–1116.

Casey, J.F., Elthon, D.L., Sikory, F.X., Karson, J.A., Sullivan, J., 1985, Geochemical and geological evidence bearing on the origin of the Bay of Island and Coastal Complex ophiolites of western Newfoundland. Tectonophysics, v. 116, p. 1-40.

Cawood, P.A. and Suhr, G., 1992, Generation and obduction of ophiolites: Constraints from the Bay of Islands Complex, Western Newfoundland: Tectonics, v. 11, p. 884-897.

Ceuleneer, G., Rabinowicz, M., 1992, Mantle flow and melt migration beneath ocean ridges: models derived from observations in ophiolites: in: JP Morgan, DK Blackman, JM Sinton eds. Mantle Flow and Melt Generation at Mid-Ocean Ridges. AGU Geophysical Monograph series, v. 71, p. 123-154.

Choi, S. H., Shervais, J. W., Mukasa, S. B., 2008, Supra-subduction and abyssal mantle peridotites of the Coast Range ophiolite, California. Contributions to Mineralogy and Petrology, v. 156, p. 551–576.

Conceição, R.V., and Green, D.H., 2004, Derivation of potassic (shoshonitic) magmas by decompression melting of phlogopite +pargasite lherzolite. Lithos, v. 72, p. 209–229.

Crocket, J. H., 2002, Platinum-group element geochemistry of mafic and ultramafic rocks. In: Cabri, L. J. (ed.) The Geology, Geochemistry, Mineralogy and Mineral Beneficiation of Platinum-Group Elements. Canadian Institute of Mining, Metallurgy and Petroleum, Special Volume 54, p. 177–210.

Dallmeyer, R.D., and Williams, H., 1975, 40Ar/39Ar ages from the Bay of Islands metamorphic aureole: their bearing on the timing of Ordovician ophiolite obduction: Canadian Journal of Earth Sciences, v. 12, p. 1685- 1690.

DeHoog, J.C.M., Hattori, K.H., Hoblitt, R.P., 2004, Oxidized sulfur-rich mafic magma at Mount Pinatubo, Philippines. Contributions to Mineralogy and Petrology, v. 146, p. 750–761.

Dick, H. J. B., and Bullen, T., 1984, Chromian spinel as a petrogenetic indicator in abyssal and alpine-type peridotites and spatially associated lavas. Contributions to Mineralogy and Petrology, 86, 54–76.

Dunning, GR, Krogh, T. E., 1985, Geochronology of ophiolites of the Newfoundland Appalachians: Canadian Journal of Earth Sciences, v. 22, p. 1659-1670.

Dunning, G.R., Chorlton, L.B., 1985. The Annieopsquotch ophiolite belt of Southwest Newfoundland; geology and tectonic significance. Geological Society of America Bulletin 96 (11), 1466–1476.

Edwards, S.J., and Malpas, J., 1995, Multiple origins for mantle harzburgites: Examples from the Lewis Hills, Bay of Islands ophiolite, Newfoundland. Canadian Journal of Earth Sciences, v. 32, p. 1046-1057.

Elthon, D., 1991, Geochemical evidence for formation of the Bay of Island ophiolite above a suprasubduction-zone, Nature, v. 140, p. 140-143.

Elthon, D, J F Casey, S Komor, 1982, Mineral chemistry of ultramafic cumulates from the North Arm Mountain massif of the Bay of Islands ophiolite: evidence for high-pressure crystal fractionation of oceanic basalts: Journal of Geophysical Research, v. 86, p. 8717-8734.

Elthon, D, J F Casey, S Komor, 1984, Cryptic mineral-chemistry variations in a detailed traverse through the cumulate ultramafic rocks of the North Arm Mountain Massif of the Bay of Islands ophiolite, Newfoundland: Ophiolites and oceanic lithosphere, v. Special Publication 13, p. 83-97.

Francis, R.D., 1990, Sulphides globules in mid-ocean ridge basalts (MORB), and the effect of oxygen abundance in Fe–S–O liquids on the ability of those liquids to partition metals from MORB and komatiite magmas. Chemical Geology, v. 85, p. 199–213.

Griffin, W. L., Zhang A., O'Reilly S. Y., Ryan, C. G., 1998, Phanerozoic evolution of the lithosphere beneath the Sino-Korean craton. In Flower M. et al. Mantle Dynamics and Plate Interactions in East Asia. American Geophysical Union, Washington, D.C., Geodynamics Series, v. 27, p. 107–26.

Harris, R.A., 1992, Peri-collisional extension and the formation of Oman-type ophiolites in the Banda arc and Brooks Range, in Parson, L.M., Murton, B.J., and Browning, P., eds., Ophiolites and their Modern Oceanic Analogues: Geological Society, London, Special Publication 60, p. 301–325.

Hattori, K.H., and Guillot, S., 2007, Geochemical character of serpentinites associated with high- to ultrahighpressure metamorphic rocks in the Alps, Cuba, and the Himalayas: Recycling of elements in subduction zones. Geochemistry, Geophysics, Geosystems, v. 8, p. 1-27.

Hattori, K., Wallis, S., Enami, M., Mizukami, T., 2010, Subduction of mantle wedge peridotites: Evidence from the Higashi-Akaishi ultramafic body in the Sanbagawa metamorphic belt. Island Arc, p. 1-16.

Ishizuka, O., Tani. K., Reagan, M. K., Kanayama, K., Umino S., Harigane, Y., Sakamoto, I., Miyajima, Y., Yuasa, M., Dunkley, D. J., 2011, The timescales of subduction initiation and subsequent evolution of an oceanic island arc. Earth and Planetary Science Letters, v. 306, p. 229–240.

Ishii, T., Robinson, P. T., Maekawah, H., Fiske R., 1992, Petrological studies of peridotites from diapiric serpentinites seamounts in the Izu-Ogasawara-Mariana forearc, Leg 125. In Fryer P., Pearce J. A., Stokking L. B., et al. Proc. ODP. Scientific Results, 125. Ocean Drilling Program, College Station, TX., 125, 445–85. doi:10.2973/odp.proc.sr.125.129.1992

Ionov, D.A., and Wood, B.J., 1992, The oxidation state of subcontinental mantle: oxygen thermobarometry of mantle xenoliths from Central Asia. Contributions to Mineralogy and Petrology, v. 11, p. 179–193.

Jenner, G.A., Dunning, G.R., Malpas, J., Brown, M., Brace, T., 1991, Bay of Islands and Little Port complexes revisited: age, geochemical and isotopic evidence confirm suprasubduction-zone origin. Canadian Journal of Earth Science, v. 28, p. 1635–1652.

Kamenetsky, V.S., Crawford, A.J., Meffre, S., 2001, Factors controlling chemistry of magmatic spinel: an empirical study of associated olivine, Cr-spinel and melt inclusions from primitive rocks. Journal of Petrology, v. 42, p. 655–671.

Karson, J. A., 1984, Variations in structure and petrology in the Coastal Complex, Newfoundland: anatomy of an ocean fracture zone. In: Gass, I. G., Lippard, S. J. & Shelton, A. W. (eds) Ophiolites and Oceanic Lithosphere. Geological Society, London, Special Publications. v. 13, p. 131-146.

Karson, J., and Dewey, J.F., 1978, Coastal Complex, western Newfoundland: An early Ordovician oceanic fracture zone: Geological Society of America Bulletin, v. 89, p. 1037–1049.

Kelemen, P.B., Joyce D. B., Webster J. D., Holloway J. R., 1990, Reaction between ultramafic rock and fractionating basaltic magma II. Experimental investigation of reaction between olivine tholeiite and harzburgite at 1150-1050_C and 5kb: Journal of Petrology, v. 31, p. 99-134.

Komor, S.C., Elthon, D. and Casey, J.F., 1985, Mineralogic variation in a layered ultramafic cumulate sequence at the North Arm Mountain massif, Bay of Islands ophiolite, Newfoundland. Journal of Geophysical Research, v. 90, p. 7705-7736.

Kurth, M, A Sassen, G Suhr, K Mezger, 1998, Precise ages and isotopic constraints for the Lewis Hills (Bay of Islands Ophiolite): Preservation of an arc-spreading ridge intersection: Geology, v. 26, p. 1127-1130.

Kurth, M-V., Sassen, A. And Galer, S., J., G., 2004, Geochemical and Isotopic Heterogeneities along an Island Arc-Spreading Ridge Intersection: Evidence from the Lewis Hills, Bay of Islands ophiolite, Newfoundland. Journal of Petrology. V. 45, p. 635-668.

Lesher C. M., Burnham O. M., Keays R. R., Barnes S. J., and Hulbert L., 2001, Trace element geochemistry and petrogenesis of barren and ore-associated komatiites. Canadian Mineralogist. v. 39, p. 673–696.

Li, C., Xu, Z., A., de Wall, S., Ripley, E. M., Maier, W. D., 2004, Compositional variations of olivine from the Jinchuan Ni–Cu sulphide deposit, western China: implications for ore genesis. Mineralium Deposita. v. 39, p. 159–172.

Mallmann, G. and O'Neil, H. St. C. 2009, The Crystal/Melt Partitioning of V during Mantle Melting as a Function of Oxygen Fugacity Compared with some other Elements (Al, P, Ca, Sc,Ti, Cr, Fe, Ga,Y, Zr and Nb). Journal of Petrology, v. 50, p. 1765-1794.

McDonough, W.F., and Sun, S.S., 1995, The composition of the earth. Chemical Geology. v. 120, p. 223-253.

Michael, P.J., and Bonatti, E., 1985, Peridotite composition from the North Atlantic; regional and tectonic variations and implications for partial melting. Earth and Planetary Science Letters, v. 73, p. 91–104.

Nell, J., and Wood, B.J., 1991, High-temperature electrical measurements and thermodynamic properties of Fe_3O_4–$FeCr_2O_4$–$MgCr_2O_4$– $FeAl_2O_4$ spinels. American Mineralogist. v. 76, p. 405–426.

Niu, Y., and Hekinian, R., 1997, Spreading-rate dependence of the extent of mantle melting beneath ocean ridges. Nature, v. 385, p. 326–329.

Pagé, P., Bédard, J.H., Schroetter, J.M., Tremblay, A., 2008, Mantle petrology and mineralogy of the Thetford Mines Ophiolite Complex. Lithos, v. 100, p. 255–292.

Pagé, P., and Barnes, S., J., 2009, Using Trace Elements in Chromites to Constrain the Origin of Podiform Chromitites in the Thetford Mines Ophiolite, Québec, Canada. Economic Geology, v. 104, p. 997-1018.

Parkinson, I.J., and Pearce, J.A., 1998, Peridotites from the Izu–Bonin–Mariana Forearc (ODP Leg 125): Evidence for Mantle Melting and Melt–Mantle Interaction in a Supra-Subduction zone Setting. Journal of Petrology, v. 39, p. 1577–1618

Parkinson, I.J., and Arculus, R.J., 1999, The redox state of subduction zones: insights from arc peridotites. Chemical Geology, v. 160, p. 409–423.

Parkinson, I.J., Arculus, R.J., Eggins, S.M., 2003, Peridotite xenoliths from Grenada, Lesser Antilles Island arc. Contributions to Mineralogy and Petrology, v. 146, p. 241–262.

Pearce, J.A., van der Laan, S.R., Arculus, R.J.,Murton, B.J., Ishii, T., Peate, D.W., Parkinson, I.J., 1992. Boninite and harzburgite from leg 125 (Bonin-Mariana forearc): a case study of magma genesis during the initial stages of subduction. In: Fryer, P., Pearce, J.A., Stokking, L.B., et al. (Eds.), Proceedings of the Ocean Drilling Program Scientific Results 125. Ocean Drilling Program, College Station, TX, pp. 623–659.

Peters, T.J., 1968, Distribution of Mg, Fe, Al, Ca and Ni in coexisting olivine, orthopyroxene and Clinopyroxene in the Totalp serpentine (Davos, Switzerland) and in the alpine metamorphosed Manlenco serpentine (N. Italy). Contributions to Mineralogy and Petrology, v. 18, p. 65-75

Puchtel, I. S., Humayun, M., Campbell, A. J., Sproule, R. A., Lesher, C. M., 2004, Platinum group element geochemistry of komatiites from the Alexo and Pyke Hill areas, Ontario, Canada. Geochimica et Cosmochimica Acta, v. 68, p. 1361-1383.

Quick J. E., 1981, The origin and significance of large, tabular dunite bodies in the Trinity peridotite, northern California. Contributions to Mineralogy and Petrology, v. 78, p. 413–22.

Righter, K., Campbell, A. J., Humayun M., Hervig, R. L., 2004, Partitioning of Ru, Rh, Pd, Re, Ir, and Au between Cr-bearing spinel, olivine, pyroxene and silicate melts. Geochimica et Cosmochimica Acta, v. 68, p. 867–80.

Sattari, P., Brenan, J.M., Horn, I., McDonough, W.F., 2002, Experimental Constraints on the sulfide- and chromite-silicate melt partitioning behaviour of rhenium and platinum-group elements. Economic Geology, v. 97, p. 385-398.

Sato H., 1977, Nickel content of basaltic magmas: identification of primary magmas and a measure of the degree of olivine fractionation. Lithos, v. 10, p. 113– 20.

Saumur, B. M., Hattori, K. H., Guillot, S., 2010, Contrasting origins of serpentinites in a subduction complex, northern Dominican Republic. Geological Society of America Bulletin, v. 122, p. 292-304.

Searle, M. P. & Stevens, R. K., 1984, Obduction processes in ancient, modern and future ophiolites. In: Gass, I. G., Lippard, S. J.&Shelton, A.W. (eds) Ophiolites and Oceanic Lithosphere. Geological Society, London, Special Publications 13, p. 303-320.

Scott, D.R., Stevenson D. J., 1989, A self-consistent model of melting, magma migration, and buoyancy-driven circulation beneath a mid-ocean ridge: Journal of Geophysical Research, v. 94, p. 2973-2988.

Shervais, J. W., 2001, Birth, death, and resurrection: The life cycle of suprasubduction zone ophiolites. Geochemistry, Geophysics, Geosystems. v. 2.

Smith, C.H., 1958, Bay of Islands igneous complex, western Newfoundland: Geological Survey of Canada Memoir, v. 290, p. 132.

Snelgrove, A. K., Roebling III, F.W., Kammara, J.L.J., 1934, The Blow-Me-Down Intrusive Complex, Bay of Islands, Newfoundland. The American Mineralogist, v. 19, p. 21-23.

Suen, C.J., Frey, F.A., Malpas, J., 1979, Bay of Islands Ophiolite Suite, Newfoundland: petrologic and geochemical characteristics with emphasis on rare earth element geochemistry. Earth and Planetary Science Letters, v. 45, p. 337–348.

Suhr, G., 1992, Upper mantle peridotites in the Bay of Islands Ophiolite, Newfoundland: formation during the final stages of a spreading centre? Tectonophysics, v. 206, p. 31-53.

Suhr, G., 1999, Melt migration under oceanic ridges: Inferences from reactive transport modelling of upper mantle hosted dunites. Journal of Petrology, v. 40, p. 575-599.

Suhr, G. & Cawood, P. A., 2001, The southeastern Lewis Hills (Bay of Islands Ophiolite), geology of a deeply eroded, inside corner, ridge transform intersection. Geological Society of America Bulletin, v. 113, p. 1025-1038.

Suhr, G., and Robinson, P.T., 2004, Origin of mineral chemical stratification in the mantle section of the Table Mountain massif (Bay of Islands Ophiolite, Newfoundland, Canada). Lithos, v. 31, p. 81-102.

Suhr, G., Batanova, V., 1998, Basal lherzolites in the Bay of Islands Ophiolite: origin by detachment-related telescoping of a ridge-parallel melting gradient: Terra Nova, v. 10, p. 1-5.

Suhr, G., Seck H. A., Shimizu N., Gunther D., Jenner G., 1998, Infiltration of refractory melts into the lowermost oceanic crust: evidence from dunite- and gabbro-hosted clinopyroxenes in the Bay of Islands ophiolite: Contributions to Mineralogy and Petrology, v. 131, p. 136-154.

Suhr, G., Cawood, P. A., 1993, Structural history of ophiolite obduction, Bay of Islands, Newfoundland: Geological Society of America Bulletin, v. 105, p. 399-410.

Tremblay, A., Ruffet G., Bédard, J.H., 2011, Obduction of Tethyan-Type Ophiolites-a Case-Study From the Thetford-Mines Ophiolitic Complex, Quebec Appalachians, Canada: Lithos, v. 125, p. 10-26.

Van der Voo, R., Spakman, W., Bijwaard, H., 1999, Tethyan subducted slabs under India Earth and Planetary Science Letters, v. 171, p. 7 – 20.

Van Staal, C. R., 2007, Pre-Carboniferous tectonic evolution and metallogeny of the Canadian Appalachians. Mineral Deposits of Canada: A Synthesis of Major Deposit-Types, District Metallogeny, the Evolution of Geological Provinces, and Exploration Methods: Geological Association of Canada, Mineral Deposits Division, Special Publication No. 5, p. 793-818.

Varfalvy, V., Hebert, R., Bedard, J.H., LaFleche, M.R., 1997, Petrology and geochemistry of pyroxenite dykes in upper mantle peridotites of the North Arm Mountain Massif, Bay of Islands Ophiolite, Newfoundland: implications for the genesis of boninitic and related magmas. The Canadian Mineralogist, v. 35, p. 543–570.

Wang, J., Hattori, K.H., Killian, R., Stern, R., 2007, Metasomatism of sub-arc mantle peridotites below southernmost South America: reduction of fO_2 by slab-melt Contributions to Mineralogy and Petrology, v. 153, p. 607-624.

Wang, J., Hattori, K.H., Stern, C., 2008, Metasomatic origin of garnet orthopyroxenites in the subcontinental lithospheric mantle underlying Pali Aike volcanic field, southern South America. Mineralogy and Petrology v. 94, p. 243-258.

Wells, P.R.A., 1977, Pyroxene thermometry in simple and complex systems. Contributions to Mineralogy and Petrology, v. 62, p. 119–139.

Whattam, S.A., Stern, R.J., 2011, The 'subduction initiation rule': a key for linking ophiolites, intra-oceanic forearcs, and subduction initiation. Contributions to Mineralogy and Petrology, v. 162, p. 1031-1045.

Williams, H., 1973, Bay of Islands map area, Newfoundland (12G). Geological Survey of Canada. Paper 72-34.

Williams, H., Colman-Sadd, S.P., Swinden, H.S., 1988. Tectonic-stratigraphic subdivisions of central Newfoundland. Paper. Geological Survey of Canada 88-1B, p. 91–98.

Wood, B.J., Bryndiza, L.T., Johnson, K.E., 1990, Mantle oxidation state and its relationship to tectonic environment and fluid speciation. Science. V. 248, p. 337–345.

Wood, B.J., and Virgo, D., 1989, Upper mantle oxidation state: ferric iron content of lherzolite spinels by 57Fe Mössbauer spectroscopy and resultant oxygen fugacities. Geochimica et Cosmochimica Acta. v. 53, p. 1277–1291.

Zagorevski, A., and van Staal, C., R., 2011, xxxxxx, [k1]IN (edited by D. Brown and P.D.Ryan) Arc-Continent Collision, Frontiers in Earth Sciences, Chapter 12. DOI 10.1007/978-3-540-88558-0_12.